12-1-2010

Modeling Light-Dark Cycle Memory in the Mammalian SCN

Benjamin L. Coffey

To the University Council:

The Thesis Committee for Benjamin L. Coffey certifies that this is the final approved version of the final electronic thesis: "Modeling Light-Dark Cycle Memory in the Mammalian SCN."

_____

Mark C. Ospeck, Ph.D.
Major Professor

We have read this thesis and recommend its acceptance:

_____

David A. Freeman, Ph.D.

_____

Mohamed Laradji, Ph.D.

Accepted for the Graduate Council:

_____

Karen D. Weddle-West, Ph.D.
Vice Provost for Graduate Program

MODELING LIGHT-DARK CYCLE MEMORY IN THE MAMMALIAN SCN

by

Benjamin Lucas Coffey

A Thesis

Submitted in Partial Fulfillment of the

Requirements for the Degree of

Master of Science

Major: Physics

The University of Memphis

December 2010

This work is dedicated to my loving wife.

ABSTRACT

Coffey, Benjamin Lucas. M.S. The University of Memphis. December 2010. Modeling Light-Dark Cycle Memory in the Mammalian SCN. Major Professor: Mark C. Ospeck, Ph.D.

The suprachiasmatic nuclei (SCN), the principal mammalian circadian oscillator, contain several thousand clock neurons that oscillate spontaneously with ~24-hour periods in its ventrolateral region. Without light, this network synchronizes through action potentials releasing VIP, compromising on a free-running period near 24 hours. We entrained Siberian hamsters to various light-dark cycles and tracked their activity into constant darkness showing that they retain memory for a particular light-dark cycle to which they were entrained before returning to their own free-running period. Using Leloup-Goldbeter mammalian clock neurons, we model the ventrolateral SCN network and show that light acting weakly upon a strongly rhythmic VIP oscillation can explain the light-dark cycle memory that we observe. Additionally, light is known to initiate a MAP kinase signaling cascade that induces transcription of both *per* and *mkp1* phosphatase. We show that the ensuing phosphatase-kinase interaction can account for the dead zone in the mammalian phase response curve.

TABLE OF CONTENTS

LIST OF FIGURES

INTRODUCTION

The extent to which most living organisms have adapted to time is often easily overlooked. In the past, many processes of organisms were simply disregarded as a passive response to the natural world. These adaptations to time provide nearly all living things with an important advantage, which is the ability to anticipate changes that occur as time moves forward. If one looks at how time is experienced on Earth, it becomes more apparent that time is the progression of rhythmic natural processes. These include tidal cycles, circadian cycles, lunar cycles, seasonal cycles, and many more. One of the most studied of these is the circadian rhythm of nearly 24 hours. This cycle of light and dark is an interesting rhythm in that the period is practically constant and yet the amount of light and darkness comprising the cycle may vary, depending upon the time of year as well as the Earth's latitude. This light-dark cycle can vary throughout the year from complete days of constant light or constant darkness, occurring at the poles, to less extreme and roughly constant days of equal amounts of light and darkness occurring near the equator.

While it can be presumed that man observed night and day behaviors in plants and animals, nothing suggests that these were considered anything more than passive responses of the plants or animals to light and/or other natural stimuli (1). Written records of the daily movement of leaves and flower petals date back to the conquest of Alexander the Great when Androsthenes made his observations at the command of Alexander himself (2). It wasn't until 1729 when Jean Jacques d'Ortous de Marian conducted an experiment and observed that the plant he was testing exhibited the same behavior of leaf opening and closing whether or not sunlight could reach it (1). In fact,

de Marian's notion of an endogenous, or internally driven, timekeeping ability was not generally accepted until over two centuries later.

Evidence now suggests that most living things possess an endogenous timekeeping ability where certain physiological processes are synchronized to occur at specific times (3). At the heart of this circadian clock (from Latin *circa* = about + *diem* = day) is a biochemical oscillation that has many features that seem to be common across species. Although there are many steps involved in the circadian oscillation, the basic theme seems to be that a gene is transcribed, translated, and eventually forms a product that will repress the gene's transcription. This product is degraded over time and with its gene turned off, repression of the gene ceases and transcription begins again, restarting the circadian cycle.

Light appears to be the principal entraining agent that synchronizes the biological clock to the circadian day (4). When not entrained and in the absence of any entraining agents, the clock's rhythmicity persists and displays a natural free-running period (FRP) close to 24 hours (5). The clock is able to adjust this FRP in response to a particular entraining agent by changing its phase (4). A reference time point (phase) is chosen with respect to the animal's internal circadian clock, which would manifest itself as an observable activity that is regulated by the clock. A second external phase is then selected for comparison. For example, in experiments conducted on Siberian hamsters entraining to a light-dark (LD) cycle, the onset of running wheel activity provides a consistent marker for clock phase and can be compared against the time of lights off. This data would then be represented as a so-called actogram shown in Fig. 1. Using an actogram, it is then possible to determine the time difference between phases (phase

angle), changes in phase (phase shifting), FRP, limits of entrainment, time to entrain, memory of entrainment, and more.

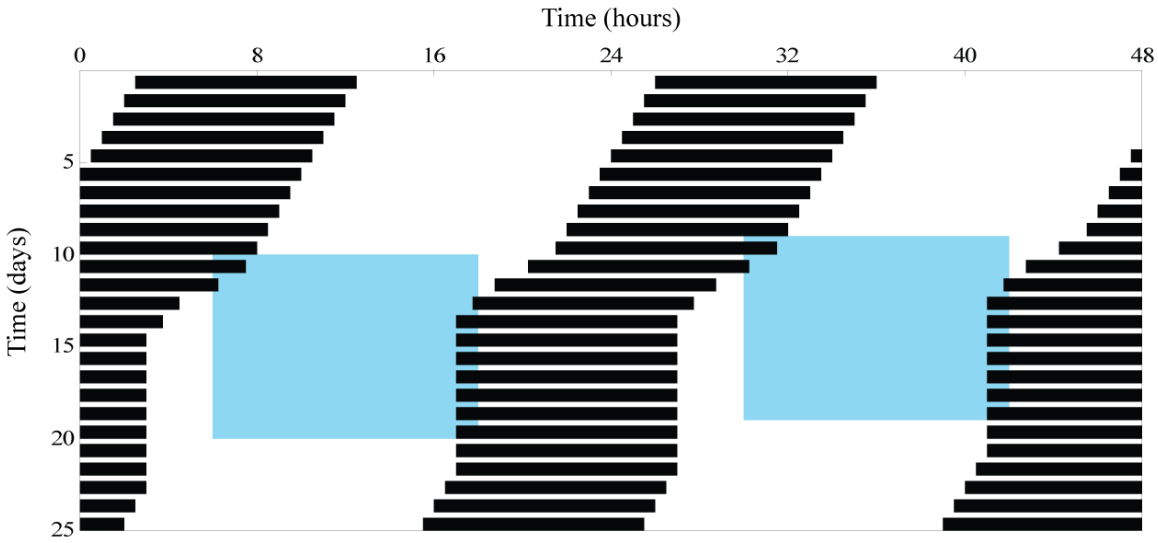

FIGURE 1 Running wheel activity can be displayed in the form of an actogram. This cartoon actogram is created by plotting running wheel activity (black bars) onto a white and blue background, representing darkness and light, respectively. It is a 48 hour double-plot meaning that the first row contains data for days 1-2, the second row data for days 2-3, the third row data for days 3-4, and so on. For the first 10 days, the animal is in constant darkness and without the presence of entraining agents, so it free-runs with a 23.5 hour period (its FRP). A typical FRP is usually near to, but not exactly 24 hours (1, 6). During day 11, the animal is exposed to a 12-12 LD cycle which causes phase advances in the activity onset during the next 4 days. Then the animal entrains for several days with a +1 hour phase angle between running wheel activity and lights off before being returned to constant darkness. The animal retains 2 days of memory for this cycle before returning to its FRP, as evidenced by no change in phase between activity onset and lights off 2 days after re-entering constant darkness.

A phase response curve (PRC) can be generated by exposing a hamster to short pulses of light at different times with respect to the onset of activity and then analyzing the resulting actogram. A PRC provides clues about the underlying mechanism of the

circadian clock and can be generated for practically any organism that displays a circadian rhythm as shown in Fig. 2 *A*-*B*.

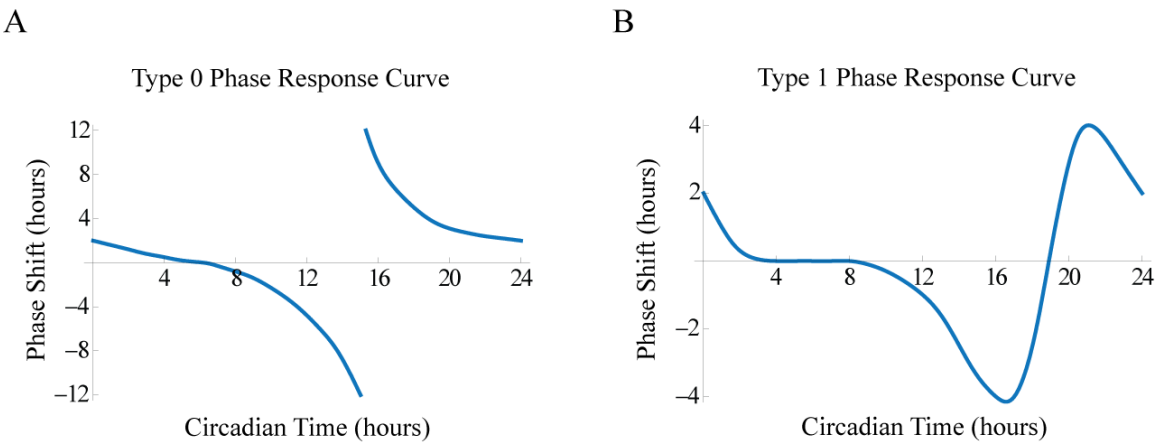

FIGURE 2 Exposure to short pulses of an entraining agent, typically light pulses, at different times with respect to a standard phase results in phase shifting by the circadian clock. The resulting data is then plotted in circadian time (CT) by scaling the FRP to a 24-hour day that has CT 0 and CT 12 denoted as activity onset for diurnal and nocturnal organisms, respectively. A negative phase shift indicates a phase delay and positive, a phase advance. CT 0-12 is known as subjective day and CT 12-24 is known as subjective night. (*A*) Simpler forms of life produce a Type 0 PRC and are capable of phase shifting up 12 hours per day. The interesting part of the Type 0 PRC is the break in the response in the early-mid subjective night in which a short amount of time separates maximum phase delay and maximum phase advance. (*B*) A Type 1 PRC is typical of more complex organisms, such as mammals which can only phase shift at most several hours per day and have dead zones, which are periods of time when an entraining agent produces no phase shift.

In the anterior hypothalamus, mammals have a pair of millimeter-sized regions known as the suprachiasmatic nuclei (SCN) shown in Fig. 3 (7). These two clusters of thousands of neurons situated behind the eyes just above the optic chiasm and in opposing hemispheres constitute the principal component of the mammalian circadian clock (3).

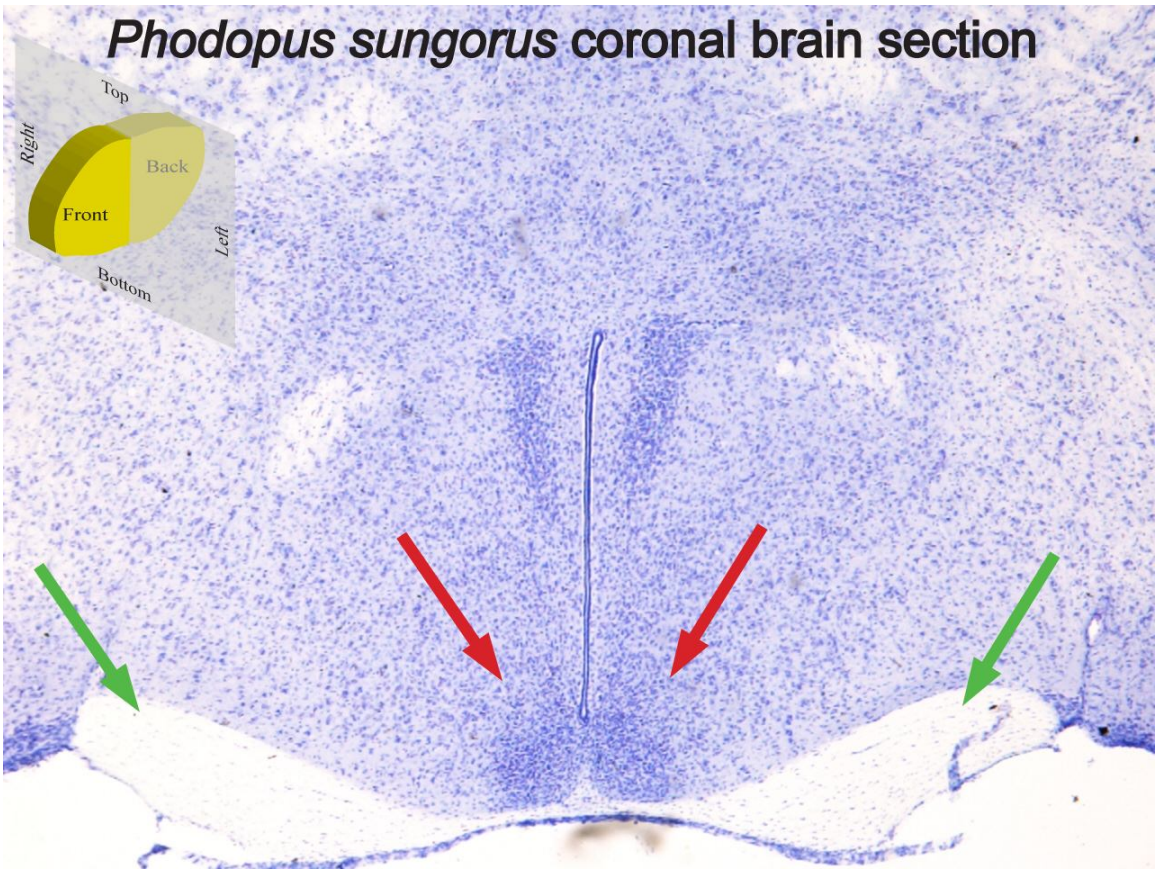

FIGURE 3 Coronal brain section of a Siberian hamster (*Phodopus sungorus*). As the inset of a coronal slice shows, the brain slice is oriented such that the reader is face-to-face with the hamster looking past the eyes into the interior of the brain. The left and right are denoting the animal's left and right. The red arrows point to the SCN which are the two areas that show up darker under staining. The green arrows point towards the optic nerves to which the stain does not adhere well to.

Rhythmic activity of SCN neurons is thought to be driven by the rhythmic expression of so-called clock genes and individual clock neurons exhibit circadian rhythms in electrical activity and gene expression *in vitro* that have independent period lengths and phases (8). SCN neurons placed at low densities in cell culture show rhythmic activity, yet they fail to synchronize together (8). However synchrony is observed in SCN slices or SCN neurons kept *in vitro* at high densities, which presumably

allows synaptic communication between them (9-10). Also, *in vitro* exposure to tetrodotoxin, a sodium channel blocker that inhibits action potentials, causes desynchronization among SCN clock neurons, suggesting that intercellular interaction via synaptic communication is necessary for synchronization to occur (9-10).

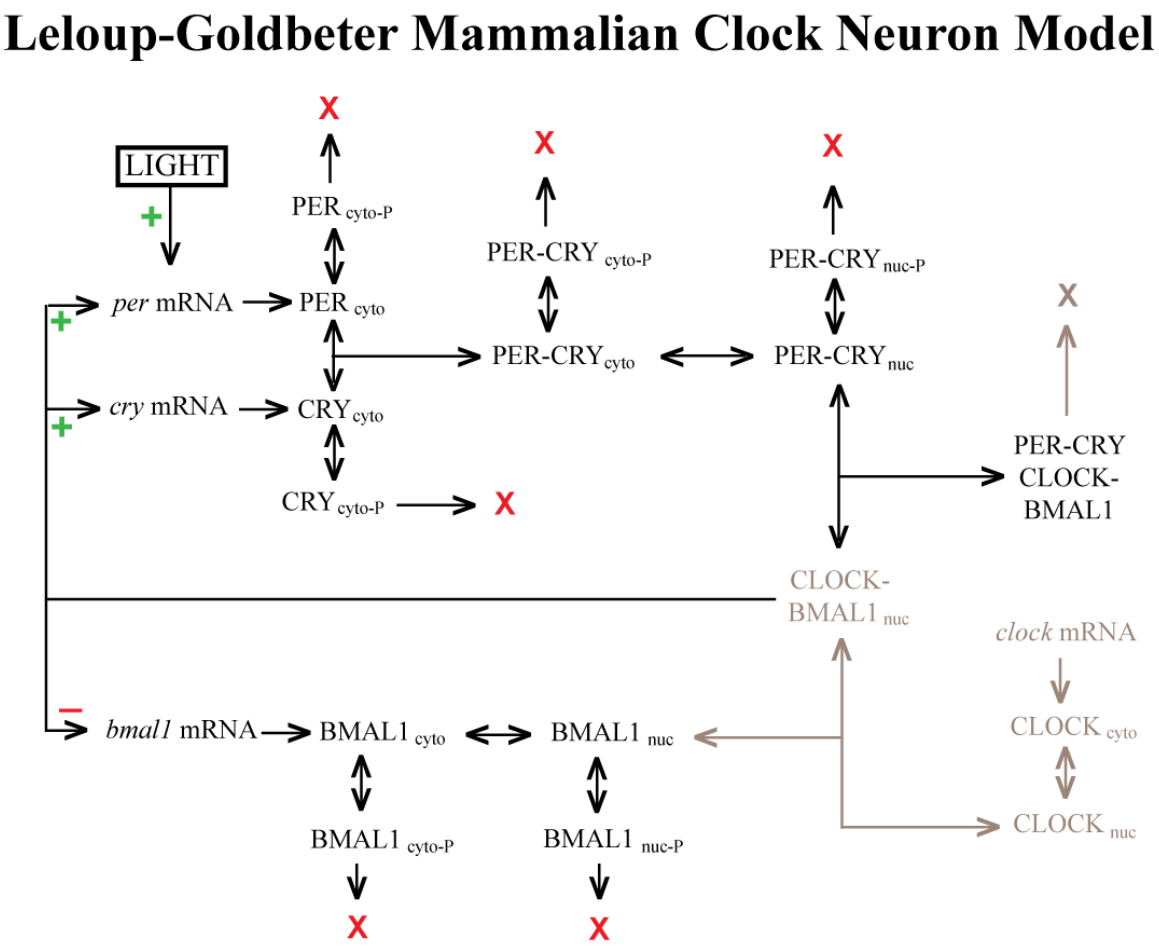

FIGURE 4 The Leloup-Goldbeter mammalian clock neuron model is a 16 dynamical variable mathematical representation of a clock neuron within the SCN that simplifies *per1*, *per2*, and *per3* into *per* and *cry1* and *cry2* into *cry*, which represent *per* and *cry* mRNAs respectively. *per* and *cry* mRNAs are translated to PER_{cyto} and CRY_{cyto} proteins, in the cytoplasm ($_{cyto}$), and then combine to form a $PER\text{-}CRY_{cyto}$ dimer which is subsequently transported to the nucleus ($PER\text{-}CRY_{nuc}$). Once there, it can trap the promoter ($CLOCK\text{-}BMAL1_{nuc}$) of the *per* and *cry* genes, preventing their transcription, thereby supplying an indirect repression upon *per* and *cry*. PER-CRY-CLOCK-BMAL1,

$PER\text{-}CRY_{nuc}$, $PER\text{-}CRY_{nuc\text{-}P}$, PER_{nuc}, $PER_{nuc\text{-}P}$, CRY_{nuc}, $CRY_{nuc\text{-}P}$, PER_{cyto}, $PER_{cyto\text{-}P}$, CRY_{cyto}, $CRY_{cyto\text{-}P}$, *per* mRNA, and *cry* mRNA make up the repressor feedback loop with ($_{\text{-P}}$) denoting that it has been marked (phosphorylated) for degradation (X). In the promoter feedback loop, the protein $BMAL1_{cyto}$, transcribed from *bmal1* mRNA, travels to the nucleus ($BMAL1_{nuc}$) where it combines with $CLOCK_{nuc}$ to form CLOCK-$BMAL1_{nuc}$ which acts to promote *per* and *cry* while also repressing *bmal1*. Evidence suggests that CLOCK is transcribed at a constant rate and does not have a circadian oscillation and thus (*clock* mRNA, CLOCK, $CLOCK_{nuc}$, and BMAL1-$CLOCK_{nuc}$) are not dynamical variables and hence are shown in gray. The repressor feedback loops is central to just about all life forms on Earth, while mammals employ two interacting feedback loops, the repressor and promoter loops.

The expression of genes that drive circadian rhythmicity in individual SCN clock neurons is accurately described by the Leloup-Goldbeter (LG) mammalian clock neuron model. In their model, the clock genes consist of *per*, *cry*, and *bmal1* which is a simplification of the known seven clock gene mechanism (3 distinct *per*, 2 *cry*, *bmal1*, and *rev-erbα*). The proteins formed from these clock genes interact to produce a sustained biochemical oscillation in constant darkness that is able to entrain to a light-dark cycle (11). Their model is described in further detail in Fig. 4.

We will show that Siberian hamsters (*P. sungorus*) form a memory for an entrained LD cycle and we will use the Leloup-Goldbeter (LG) clock neuron model as a stepping stone to a biophysically-based model of the mammalian SCN that is able to account for this light-dark cycle memory.

METHODS

Experiments were conducted in compliance with The University of Memphis IACUC Animal Research Protocol. Siberian hamsters, *Phodopus sungorus*, were our model organism and were placed into individual cages fitted with running wheels wired

to provide a voltage spike per revolution of the wheel that was recorded by a computer operating Windows XP. Clocklab data collection and analysis software (Coulborn Instruments, Allentown, Pennsylvania) was used to collect data, control light-dark cycles (LD cycles), create actograms, as well as to analyze the data. Each actogram was analyzed to obtain a linear fit to the onset of a particular animal's running wheel activity. Animals were exposed to florescent and incandescent lights for the various LD cycles that were tested. Four fluorescent light bulbs provided approximately 11,000 Lumens of flux and gave about 2000 candles per square meter and similar results were obtained from the two 11 watt incandescent bulbs. In order to calculate the number of days of LD cycle memory, we made two fits to activity onset (Fig. 5 *G-H*.). The first fit used data during the LD cycle and determined entrainment, whereas the second fit used data from when the animal returned to constant darkness and determined the its FRP. The range of data for the first fit was then extended to include days in constant darkness. Due to the relatively few days of data during entrainment for the first fit, including days for which the animals had no memory for the LD cycle would cause a noticeable increase in its standard deviation.

EXPERIMENT

The aim of these experiments was to test Siberian hamsters' memory for a particular LD cycle and also their limits of entrainment. This involved exposing them to a light-dark cycle for several days until they entrained. After entrainment, they were subjected to constant darkness in order to record how long it would take before they reverted back to their own free-running period (FRP).

To test for memory of a light-dark cycle, two types of 24-hour LD cycles were used with the first being static and following the form XLYD. For example, 10L14D meant 10 hours of light was followed with 14 hours of darkness similar to static LD cycles near a solstice. The second "moving" light-dark cycle involved converting each day a set interval of time from light to dark, or vice versa, starting from an initial LD cycle (similar to the changing conditions near an equinox). This change in LD cycle was always enacted at lights off (phase advance = lights off earlier each day; phase delay = lights off later each day). This LD cycle is expressed in the form XLYD±Z with Z being the changing interval of time in hours. For example, 15L9D-0.25 meant the first day was 15 hours of light and followed with 9 hours of darkness and then involved converting 15 minutes, 0.25 hours, of light into 15 minutes of darkness each consecutive day (note that this causes a phase advance of the light-dark edge and activity onset for a nocturnal animal). During these cycles, light onset occurred at the same time each day, whereas light offset would vary accordingly. This method was used because Siberian hamsters, being nocturnal, display much more consistent activity during the light offset, or the sunset portion of their cycle. The next day's onset of running wheel activity can then be predicted to within a span of just a few minutes. Of 57 hamsters, 31 entrained to a 24-hour LD cycle with an average LD cycle memory of 2.0 ± 0.3 days (12). Using a p-test, with a null hypothesis that hamsters formed no memory of the light-dark cycle, obtained a p-value of $\sim 10^{-7}$, soundly rejecting the null hypothesis. Hence, it is virtually impossible for the animals not to have formed a memory for a particular LD cycle with a period length close to 24 hours (12). Actograms are shown in Fig. 5 *A-D* for some of the LD cycles that were used.

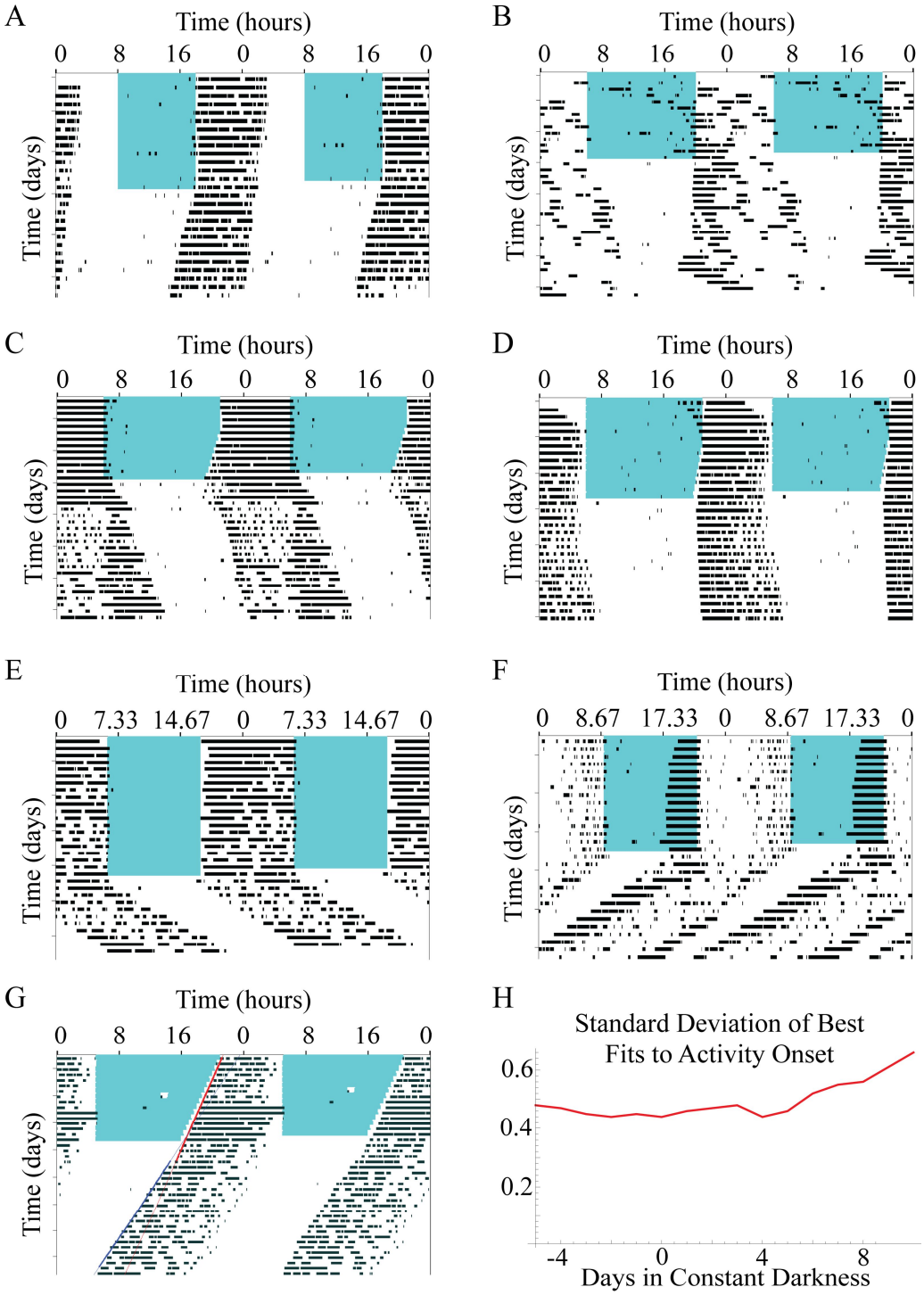

FIGURE 5 Siberian hamsters were housed individually in cages while their running wheel activity was recorded. They were placed into light-dark cycles before being allowed to continue into constant darkness for several days. Linear least-squares fits to

activity onset are used in order to quantify the number of days of memory an animal retains for a particular LD cycle. (*A*) Animal shows ~2 days of memory after entrainment to a 10L14D. (*B*) Animal shows ~2 days of memory after entrainment to a 14L10D. (*C*) Animal entrained to a 16L8L-0.25 shows ~3 days of memory. In this LD cycle the light offset is phase-advanced by 15 minutes per day for 7 days. (*D*) Animal shows ~2 days of memory when entrained to a 16L8D-0.17, which phase-advances the light offset by 10 minutes per day for 7 days. (*E*) The animal in an11L11D shows ~1 day of memory for the LD cycle simulating a 22 hour day. (*F*) While in a 13L13D, simulating a 26 hour day, the animal retains ~1 day of memory. (*G*) This animal was entrained to a 16L8D-0.33, which phase-advanced light offset by 20 minutes per day for 15 days, and showed ~4 days of memory. A linear fit to the animal's activity onset during the LD cycle (red) determines entrainment and a second linear fit during the constant darkness phase (blue) determines the FRP. To calculate how many days of memory an animal has for a particular LD cycle, the entrainment fit is extended to include days after being returned to constant darkness. (*H*) An increase in the standard deviation of the fits occurs when more days are included into the first fit beyond the number of days an animal has a memory of entrainment. This is due to the fit not having a large number of days of data, so that one day that deviates (no memory) included in the fit produces a recognizable increase in standard deviation. This animal had about 4 days of memory of the LD cycle as seen by the increase in standard deviation after the fourth day in constant darkness.

To test the limits of entrainment of Siberian hamsters, a relatively small set of non-24-hour LD cycles were used, specifically, simulating day lengths from 20 hours to 28 hours. Those beyond 22 to 26-hour day lengths seemed to be too extreme for entrainment. Of the 9 Siberian hamsters that entrained within the previously mentioned range, the average cycle memory was reduced to 0.8 ± 0.15 days (12). Using a p-test with the null hypothesis that hamsters form no memory for a close-to-24-hour LD cycle obtained a p-value of ~0.0004, again rejecting the null, and confirming that they form a somewhat lesser memory for a cycle with a period length relatively close to 24 hours (12). Actograms are shown in Fig. 5 *E-F* for some of the LD cycles that were used.

MODEL

The mammalian SCN is not uniform in its organization and structure; hence this compartmentalization must be taken into account in order to construct a model that can simulate its entrainment properties. Since its ventrolateral (VL) region is thought to be primarily responsible for the synchronization of the entire organ; it will be the focus for the model (9-10, 13). Neurons in the VL region of the SCN are well characterized by the Leloup-Goldbeter (LG) mammalian clock neuron model, which was mentioned in the introduction, thus we couple together a network of these to model the VL SCN. Note that due to computational limitations, we employ a reduced-dimension LG model neuron, discarding its six degradation pathways, while still maintaining functionality similar to the original. The resulting reduced-dimension LG model neuron, shown in Fig. 6 *A*, is 10 dimensions and still includes the repressor and promoter feedback loops.

In the resulting LG neuron network, our model neurons exchange vasoactive intestinal polypeptide (VIP) because it is well known that the VL SCN employs this neuropeptide as a synchronization factor (9, 14). VIP concentration locks itself to a circadian oscillation during entrainment to a 12-12 light-dark cycle and experiences a similar, but smaller oscillation in constant darkness (15). Also, light acts to slowly damp a neuron's VIP production with an ~8 hour time constant and when VIP exchange in the SCN is high, its concentration continues to decrease (15). Additionally, VIP is known to depolarize a clock neuron by ~12 mV and to initiate a membrane potential oscillation, both of which act to increase firing rate and in turn VIP exchange (16-19). All of the above suggest including a ~12 hour negative feedback loop in which VIP production is slowly damped in a clock neuron by the VIP that it receives from other clock neurons.

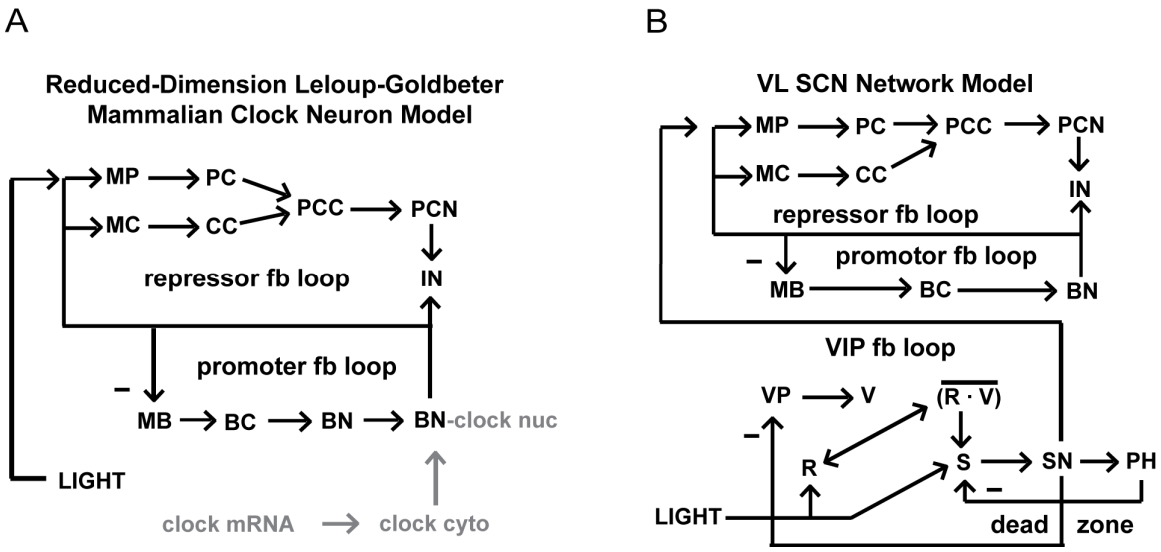

FIGURE 6 (*A*) The Leloup-Goldbeter (LG) mammalian clock neuron model. In the reduced-dimension version of the LG model neuron, the degradation pathways have been discarded (compare to Figure I4.). The variables comprising the repressor feedback loop consist of *per* and *cry* mRNAs (MP and MC), per and cry proteins (PC and CC), per-cry protein dimer (PCC), and nuclear per-cry protein dimer (PCN) which act to repress the production of MP and MC. The variables comprising the promoter feedback loop consist of *bmal1* mRNA (MB), bmal1 protein (BC), and nuclear bmal1 protein (BN) which acts to promote the production of MP and MC. The variable linking the two feedback loops is clock-bmal1-per-cry tetramer (IN) which indirectly inhibits MP and MC production. In the LG model neuron CLOCK protein is not a dynamic variable and is colored gray to represent its relatively constant levels. (*B*) The mammalian VL SCN network model consists of LG clock neurons each of which is described by 16 variables and 4 feedback loops. The model incorporates the promoter and repressor feedback loops and contains two additional feedback loops. In constant darkness an oscillation in the neuropeptide VIP (V) and its precursor (VP) drives oscillations in firing rate (R), which peaks near CT7, and in second messenger (S) which causes per mRNA (MP) to peak near CT8, synchronizing the network (20-21). Feedback loops are internal within a single clock neuron except that in the VIP loop, it is the average rate of receiving VIP from other clock neurons (average product of R and V) which sets target firing rate and second messenger. Light acts on both firing rate and second messenger within this loop to induce *per* mRNA within about one hour (20). The dead zone where the network is insensitive to phase-shifting by light can be accounted for by a strongly nonlinear phosphatase-kinase (PH-S) interaction.

It is known that 15 minute light pulses act to sharply increase *per* mRNA concentrations within about an hour and also that *per* peaks around CT 8 (20) with an animal entrained to an LD cycle. Retinal ganglion cells exposed to light increase their firing rate and this results in increased VIP exchange between clock neurons (22). Received VIP initiates multiple signaling pathways, some of which leading to the activation of CREB (21, 23-24). This nuclear transcription factor then binds to a specific sequence of DNA to up-regulate clock gene transcription, specifically inducing *per* mRNA.

Clock neuron firing rates also experience a circadian oscillation in constant darkness, approximately doubling during the subjective day and peaking around CT 7 (25). Interestingly, the hyperpolarizing neurotransmitter GABA is cotransmitted together with depolarizing VIP and clock neuron firing rates tend to be very slow ($\leq$ 10 Hz). We assume that one purpose of GABA cotransmission is to limit the increase in firing rate when a clock neuron receives VIP so that during subjective day when GABA exchange is relatively high it causes firing rate to saturate. Note SCN neurons are approximately three times more likely to increase their firing rate during subjective night when it is low as compared with subjective day (26). Together these findings lend support to the hypothesis that in constant darkness an oscillation in VIP should be able to drive both firing rate and *per* transcription so as to synchronize the network.

It has been shown that an acute light-dependent increase of *per* mRNA in a mouse can result via a pathway that is independent of VIP (21, 23-24, 27). Part of this the mechanism involves a kinase being translocated to the nucleus where it phosphorylates CREB which then acts independently of the clock/bmal1 promoter to induce both *per* and

mkp1 transcription (28). It is assumed that this pathway acts in parallel with the VIP pathway to promote *per* transcription (see Fig. 6 *B*). It would seem that VIP is forcing a *per* oscillation in constant darkness and phase shifting is caused by light-induced *per*.

The model of the mammalian VL SCN network consists of clock neurons that are described by 16 dimensions with the first 10 coming from a reduced Leloup-Goldbeter mammalian clock neuron model. Added to these are 6 dimensions that take into account firing rate and VIP exchange among the neurons in the network. Each neuron's 16 variables are associated with 16 first order differential equations that describe the time rate of change of each variable. Figure M1.B. shows a clock neuron of the mammalian VL SCN network model and the interactions between variables. The following list describes each variable (corresponding to a differential equation that can be found in the appendix).

Six variables account for the repressor feedback loop:

1. *MP* = per mRNA, inhibited by nuclear per-cry dimer (*PCN*), promoted by nuclear clock-bmal1 (*BN*) and independently by phosphorylated CREB (*SN*)
2. *MC* = cry mRNA, inhibited by nuclear per-cry dimer, promoted by nuclear clock-bmal1
3. *PC* = cytoplasmic per protein
4. *CC* = cytoplasmic cry protein
5. *PCC* = cytoplasmic per-cry protein dimer
6. *PCN* = per-cry dimer in the nucleus, which binds clock-bmal1 (*BN*) to repress per, cry transcription

Three variables account for the promoter feedback loop:

7. *MB* = bmal1 mRNA, inhibited by nuclear bmal1 (*BN*) protein. In the LG model clock is transcribed at a constant rate so that clock protein is considered an implicit part of bmal1 (B).

8. *BC* = cytoplasmic bmal1 protein

9. *BN* = nuclear bmal1 protein; inhibits *MB*, promotes per and cry transcription.

One variable accounts for the coupling of the repressor and promoter feedback loops:

10. *IN* = nuclear inhibitor of per and cry transcription. Inhibitor is made when per-cry (*PCN*) dimerizes to clock-bmal1 (*BN*) thus preventing it from promoting per and cry transcription.

Negative feedback loop in which received VIP damps a clock neuron's own VIP production, resulting in an endogenous VIP oscillation in constant darkness:

11. *VP* = VIP precursor, inhibited by received VIP

12. *V* = VIP neuropeptide exchanged between clock neurons in the ventrolateral SCN

13. *R* = clock neuron firing rate. When low it is quickly increased by received VIP, but when *R* is high we assume that the GABA cotransmitted along with VIP causes the firing rate to saturate.

14. *S* = phosphorylated MAP kinase in the cytoplasm caused by VIP binding to the VPAC2 receptor

15. *SN* = nuclear CREB presumably turned on by MAP kinase, which then induces per and mkp1 transcription. Our assumption is that it also damps VIP precursor (*VP*).

16. *PH* = mkp1 phosphatase induced by CREB (*SN*) that dephosphorylates/shuts off MAP kinase signal (*S*).

In constant darkness the SCN is able to form a synchronized free-running period (FRP) that varies from animal to animal, but is usually within a half hour of 24 hours long (11, 22). Individual neurons within the SCN have a wide variance in the natural period of their repressor and promoter feed back loops, with period lengths that range between 22-28 hours (11). So as to obtain a distribution of natural periods within the network we used a Gaussian-distributed random variable s_i as a scale factor that multiplied all the rate constants for the repressor and promoter feedback loops inside a given neuron. Rate constant noise in the VIP feed back loop is not included, although small amounts of it produced similar results. Also, while the VL SCN includes several thousand neurons, computational limitations allow for simulating all-to-all coupling between 50 neurons for times less than 1000 hours on a PC. Simulations were run using Mathematica 5.2 on a Dell computer with a Microsoft Windows XP operating system and an Intel Pentium 4 processor (model in support file). A basic model was constructed where light causes a fast increase in second messenger (S) which induces both *per* and phosphatase transcription. Induced *per* phase shifts the repressor feed back loops inside the clock neurons while high levels of phosphatase block further second messenger signal and establish a dead zone where the clock neurons become insensitive to phase-shifting by light.

RESULTS

A network of LG model clock neurons can be coupled together through the exchange of the neuropeptide VIP. When VIP is made to oscillate in a 12 hour negative feedback loop (Eqns.11-15; *VP, V, R, S, SN*) received VIP causes fast *per* transcription

which synchronizes all the repressor loops together in constant darkness (Eqn.1; Fig. R1. A.). This synchronization depended on several factors, first that received neuropeptide would quickly increase firing rate together with per transcription, second that received neuropeptide was slowly coupled back to inhibit neuropeptide precursor and third that this feedback loop needed to be strongly rhythmic. Strong rhythmicity in turn depended on received VIP inhibiting a clock neuron's own VIP production through a high gain, nonlinear negative feedback (Eqn. 11).

The model was able synchronize itself in complete darkness by using part of the second messenger pathway that is employed for entrainment to light. In general, the compromise frequency struck between coupled nonlinear oscillators can be either greater than or less than their average frequency, as it depends on the relative strengths of the couplings from the fast oscillators to the slow ones and vice versa (29), and a good example of this would be phaselocking between fire flies (30-31). In the case of the SCN it is possible that the coupling between neurons acts to slow the network down and lengthen its natural period above the average period of the neurons (32-34). Here it is the time constant for the VIP feedback loop which sets the network compromise period and we chose it to be very close to the average period (24.0 hours) of the model neurons, although it could be adjusted to either speed up or slow down the network.

Electrically we consider a clock neuron as a small capacitor with a voltage threshold that when surpassed results in an action potential. VIP received from other clock neurons increases membrane potential and firing rate, while received GABA has the opposite effect, decreasing membrane potential and firing rate. Firing rate is also increased by positive leak conductance turned on by retinal ganglion cells that are

exposed to light. Thus our target firing rate is proportional to the average firing rate-VIP product when it's small, but then saturates due to the cotransmission of GABA when this product becomes large, and also includes a step function representing input from retinal ganglion cells that are exposed to light (Eqns.13, 13a).

We obtained a phase response curve (PRC) for the synchronized network where a pulse of light was represented by two step functions that immediately increased both the rates of change of firing rate and of second messenger. Then by adjusting the strength of these light induced increases in dR/dt and dS/dt the recorded phase shifts due to 15 minute light pulses could be made similar to PRCs obtained from mammalian experiments (22, 35; Figure R1. F.). Physically, light causes the transmission of glutamate and PACAP along axons of the RHT to the VL SCN so that it is logical that the light-induced second messenger (*S*) is in part due to PACAP binding to the $VPAC_2$ receptor (36). Also it is now known that acute light-dependent increase of *per* mRNA in mouse can result via an NMDA receptor pathway that is independent of VIP and the $VPAC_2$ receptor (27). Meanwhile VIP (*V*) is being continuously exchanged between clock neurons so our second messenger target was proportional to the average firing rate-VIP product plus a step that we attribute to light-induced input from retinal ganglion cells (Eqns.14, 14a). Light induced increases in firing rate also act to increase *S*.

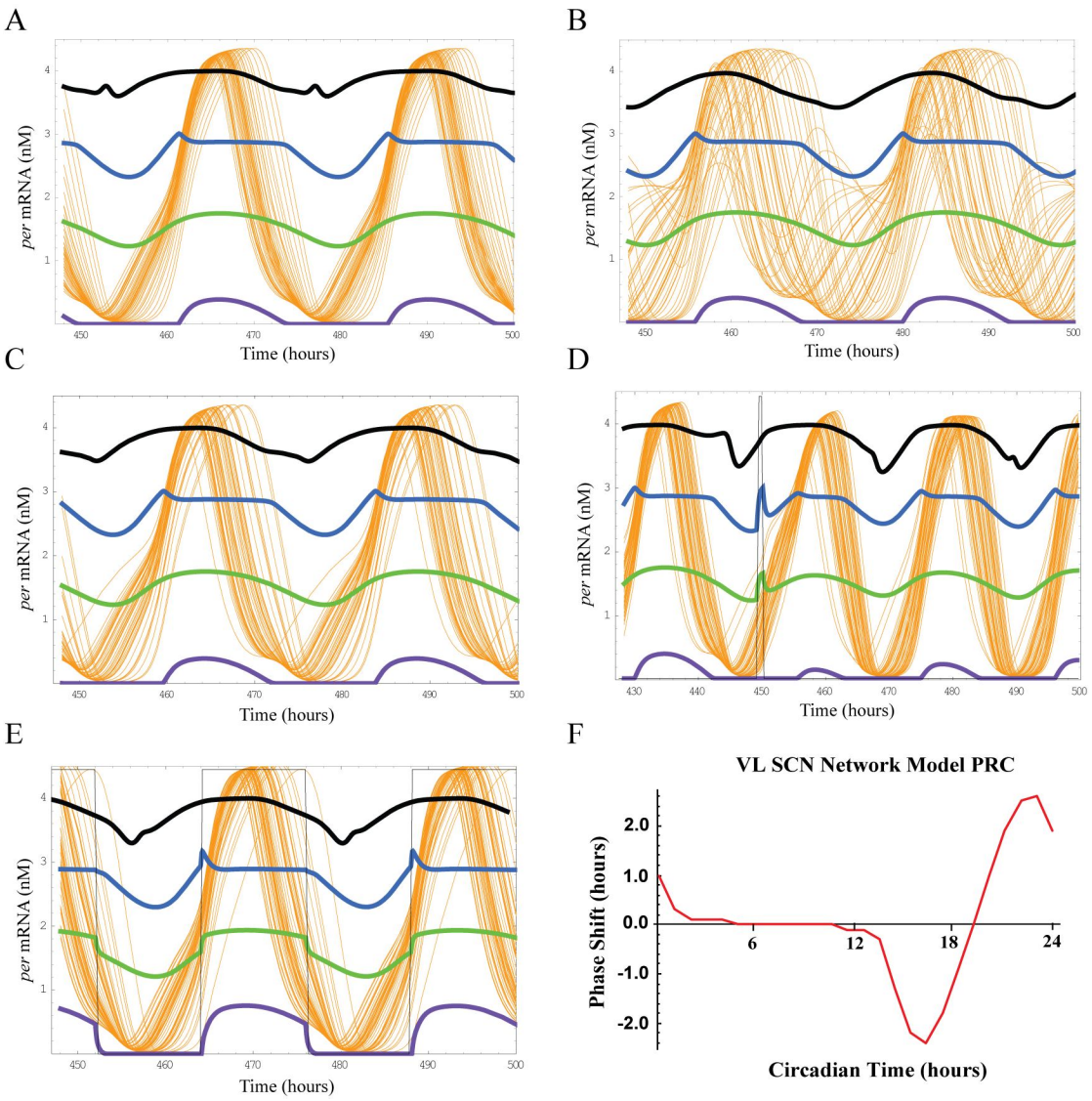

FIGURE 7 (*A*) The VL SCN network model forms a compromise free-running period (FRP) for 50 neurons in complete darkness. *per* mRNA (orange) oscillates in the dark from ~0-4 nM. The four overlaid curves are each scaled 0-1. On top is synch order parameter (black) *synch* = $\frac{\text{variance}_{\text{time}}\left[\text{mean}_{\text{neuron i}}\left[\text{MP}_{\text{i}}\right]\right]}{\text{mean}_{\text{neuron i}}\left[\text{variance}_{\text{time}}\left[\text{MP}_{\text{i}}\right]\right]}$, where 1.0 is perfect synch and 0.0 is no synch, although it should be noted, due to its placement, 4.0 and 3.0 represent 1.0 and 0.0 (32, 39). A scaled second messenger signal (blue), MAPK *S*, occupies the 2.0-3.0 region in the y-axis. The scaled firing rate (green), *R*, which oscillates by an approximate factor of two, occupies the 1.0-2.0 region. Finally, the deadzone (purple) is at the bottom. The repressor and promoter feedback loops for 50 clock neurons synchronize together in constant darkness through the exchange of VIP. Neurons are given a Gaussian distribution in the period lengths of their repressor and promoter feedback loops with an average period of 24.0 hours and a standard deviation of

1.2 hours. (*B*) The effect of a greater standard deviation (2.4 hours) in the individual FRPs of clock neurons is that the network struggles to maintain a compromise FRP. (*C*) When the amount of noise in the VIP feedback loop is doubled, VIP is still able to synch the network during high intracellular VIP exchange. (*D*) When exposed to a pulse of light (1 hour, *ptrbR* = 0.06, *ptrbS* = 0.06, thin black spike), the network phase delays ~ 1 hour. Repeating the process at different circadian times will produce a phase-response curve (PRC). (*E*) The network is entrained to a 12-12 LD cycle with the rectangles indicating when the lights were on. (*F*) Phase response curve constructed by measuring the model network's phase shift due to a 15 minute pulse of light in constant darkness (light pulse represented by *ptrbR* = 0.04 in Eqn.13 and *ptrbS* = 0.08 in Eqn.14).

The generic PRC includes an interesting region about 9 hours long called the dead zone where the mammal is insensitive to phase-shifting by light (22). Unlike the mammal, fruit fly clock neurons see the light, which acts directly through chromophore within them to degrade clock proteins and induce phase shifts (37). Clock protein concentration oscillates so that when it is low the fly becomes insensitive to phase-shifting by light. However, phase-shifting and dead zone in mammals must work by a different principle since mammalian clock neurons are kept from seeing sunlight directly and their clock proteins are known to peak during the late part of the dead zone. In the mammal, instead of degrading clock proteins, light induces transcription of both *per* and *mkp1* phosphatase (20, 24). It's interesting that light uses cAMP/PKA, Ca^{2+} and MAP kinase signaling pathways for this gene induction and that one of the induction targets is a phosphatase which dephosphorylates MAP kinase. This interaction between kinase and phosphatase is known to be very strongly nonlinear and we hypothesize that it is responsible for the dead zone (38; exponent q=50 step function in Eqn.14b). Light causes an increase in phosphorylated kinase signal which is followed by the induction of dephosphorylated phosphatase. Kinase phosphorylates the phosphatase, changing its

conformation so that it will dephosphorylate future kinase signal (38). Thus whenever the kinase-phosphatase product exceeds a certain threshold it will establish a dead zone. The interaction acts to truncate the phosphorylated kinase signal (Fig. 7 *A-E*.) and effectively would make the SCN into a light-edge detector.

In constant darkness our simulated dead zone is generic and about 9 hours long (22). Note there is experimental evidence that the width of the Siberian hamster's dead zone shortens to ~7 hours after the animal has been entrained to a winter 9-15 light-dark cycle (35), the implication being that cycle memory makes the dead zone into a dynamic rather than static interval. We note that in our simulations the dead zone expands to ~12 hours after entrainment to a summer 16-8 light-dark cycle. However our simulated dead zone does not shorten after entrainment to a winter 8-16 cycle, but would if short day lengths were to down regulate VIP to second messenger signaling *S*. Also, there is recent experimental evidence for something like a kinase-phosphatase mechanism as being responsible for the dead zone. Without $VPAC_2$ signaling the mouse SCN becomes inappropriately responsive to phase-shifting by light during the day, the implication being that VIP signaling is responsible for the dead zone (27). In their experiment light via an NMDA pathway was able to acutely induce *per* during the supposed dead zone for the *Vipr2-/-* mutant mouse whose *mPer1* mRNA (and presumably also *mkp1* mRNA) remained low throughout the circadian day. In our model it is VIP-driven *mkp1* induction which is responsible for the dead zone.

We tested the model's ability to entrain to the circadian day by using step functions to make sequences of light periods. The network had a free running period of 24.0 hours and was able to phase shift by 10-12 hours in 6-7 days, advancing or delaying

to acquire lock to a 12:12 light-dark cycle (Fig. 8 *A-D*). Increasing or decreasing the coupling strength between light and the network respectively decreased or increased the time to acquire the cycle. The coupling strengths *ptrbR* = 0.006 in Eqn.13 and *ptrbS* = 0.006 in Eqn.14 were chosen to be consistent with time-to entrain, cycle-memory and limits-of-entrainment experiments.

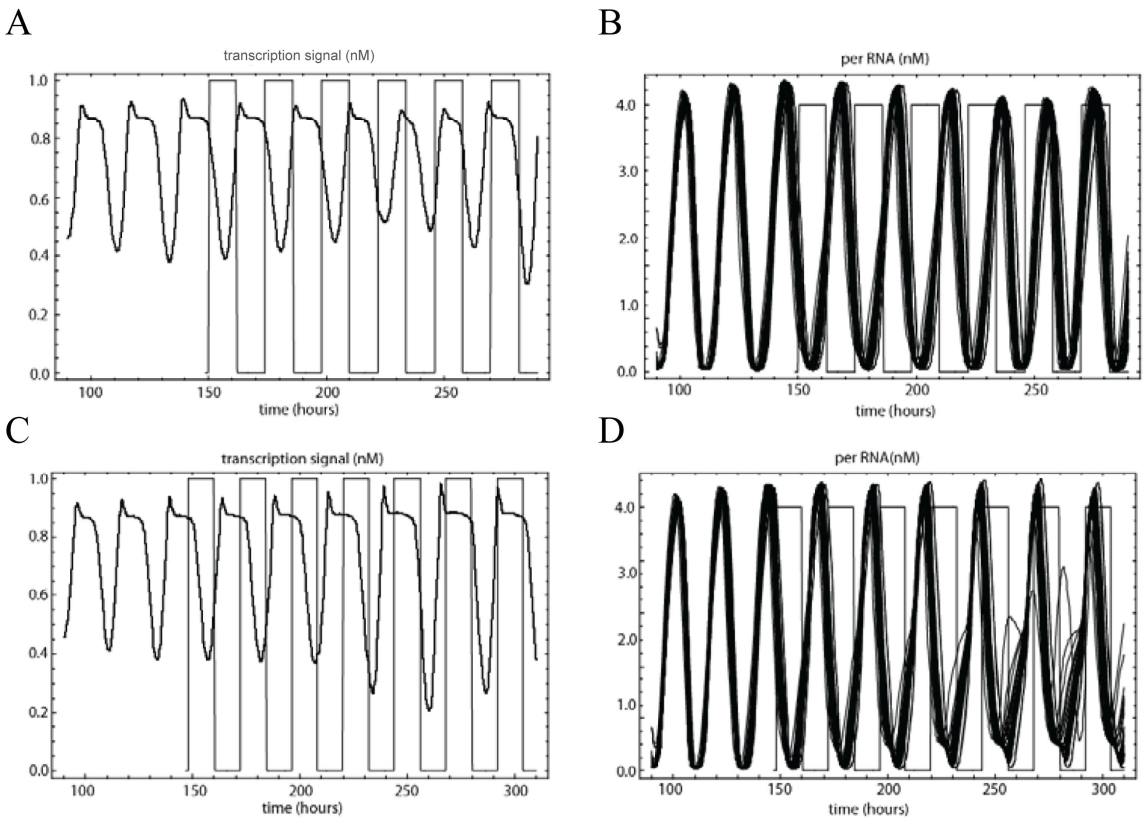

FIGURE 8 Entrainment of the model network to a sequence of 12-12 light-dark cycles. It takes approximately 6 days to phase advance by about 12 hours to entrain the (*A*) transcription signal (*SN*) and (*B*) *per* RNA (*MP*). It takes about 7 days for a 10 hour phase delay to entrain the (*C*) transcription signal and (*D*) *per* RNA. Light periods are shown as sequences of black rectangles and represented by *ptrbR* = 0.006 in Eqn.13 and *ptrbS* = 0.006 in Eqn.14.

Next we investigated the model's memory for the particular light-dark cycle to which it was entrained together with its limits of entrainment. Fire flies are known to have a resetting strength where a larger strength permits synchronization between two flies with more dissimilar frequencies (29). Here the coupling is between a network with a 24.0 hour free running period and a specific light-dark cycle. Our light periods are defined by the height of the step changes they make in dR/dt and dS/dt (*ptrbR* = 0.006 in Eqn.13 and *ptrbS* = 0.006 in Eqn.14). This choice permitted the network to entrain cycle lengths between about 22-26 hours, while our experimental range of entrainment was 20-26 hours (Fig. 9 *A*-*B* and *E*-*F*). While holding day length constant we locked the network to various light-dark cycles. When fixed to a 24 hour day length the model was able to remember the particular cycle, i.e. 10-14, 14-10, etc. that it was locked to while proceeding into constant darkness (Fig. 9 *C*-*D*). Cycle-rate memory tests began with 12-12 light-dark cycles which for 12 days increased or decreased their light period by 10 minutes per day in order to mimic large day length changes that occur at high latitudes near to an equinox (40). Again, similar to our experimental animals the model was able to anticipate the expected light and dark edges while proceeding into constant darkness (Fig. 9 *G*-*H*).

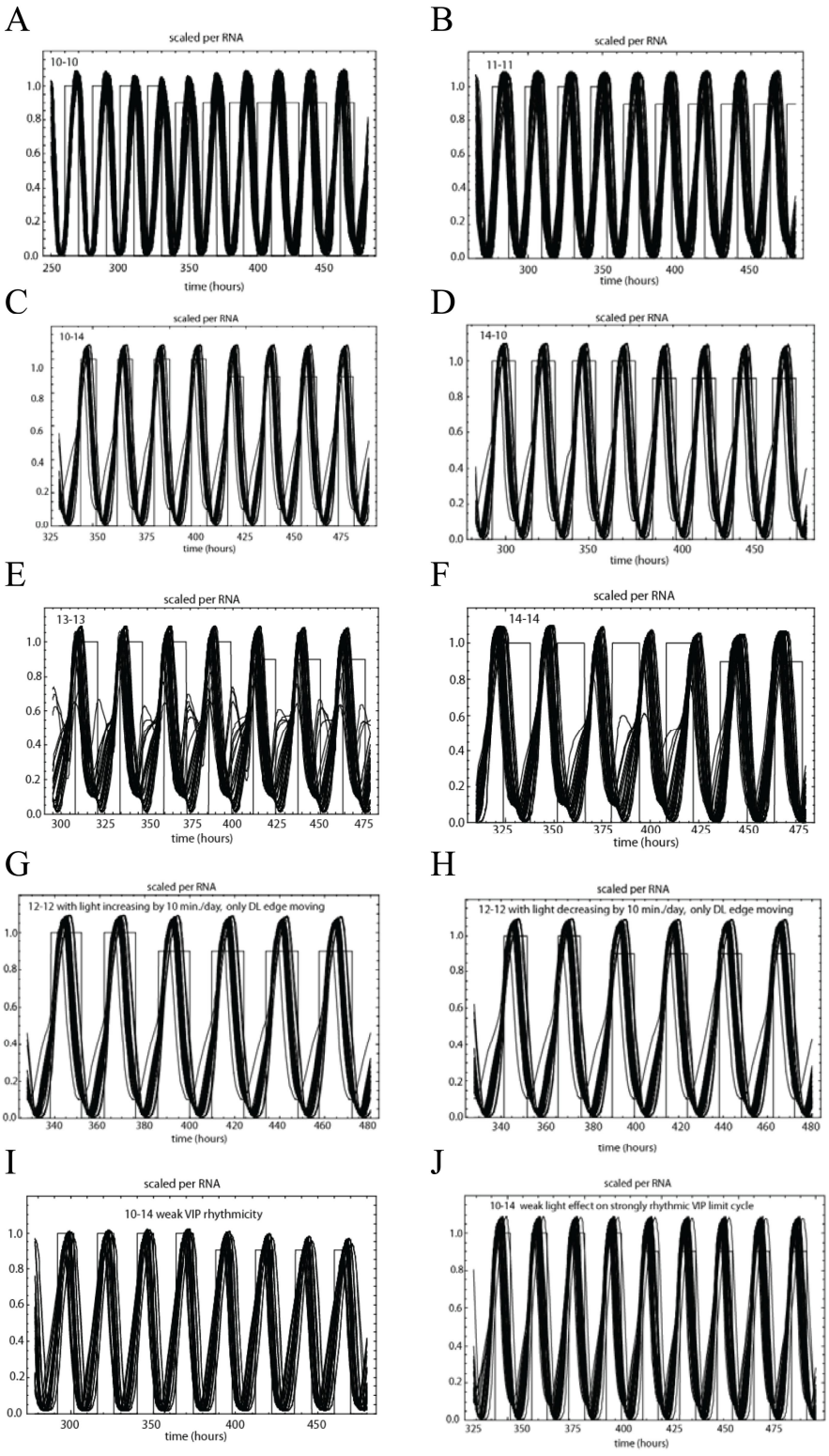

FIGURE 9 Light-dark cycle memory and range of entrainment. *per* RNA (*MP*) is shown for the last several of 12 days of light-dark cycles. Periods of light are indicated by the

tall rectangles, while the shorter rectangles are in constant darkness and show where the light would be if the cycle were continued. PS1, 2, 3 are the network phase shifts for the first, second and third days in constant darkness with respect to the last day on the cycle. (*A*) Model with a free running period of 24.0 hours was unable to lock a 10-10 cycle (*B*) able to lock an 11-11 cycle (PS1= 0, PS2=-119 min., PS3 =-200 min). (*C*) 10-14 cycle had one day of memory before phase advance (PS1= 0, PS2= +13 min., PS3 = +13 min). (*D*) 14-10 cycle one day of memory before phase delay (PS1= 0, PS2=-47 min., PS3 =-47 min). (*E*) 13-13 cycle had one day of memory before phase advance (PS1= 0, PS2= +30 min., PS3 = +54 min). (*F*) unable to lock 14-14 cycle. (*G*) 12-12 cycle whose light was advanced/increased by 10 minutes per day shows about one day of cycle-rate memory before phase delay (PS1= 0, PS2=-32 min., PS3 =-47 min). (*H*) 12-12 cycle who's light period was delayed/decreased by 10 minutes per day also had one day of cycle-rate memory before phase advance (PS1= 0, PS2= +32 min., PS3 = +32 min). (*I*) Memory lost for 10-14 cycle when rhythmicity of the VIP oscillation reduced (*c4* 0.37 → 0.36 in Eqn. 11, *c9* 1.5 →1.45 in Eqn. 13a, *c11* 2.0 →1.5 in Eqn 14a, *s* 0.96 → 0.88 to maintain 24.0 hour period; PS1= -15 min., PS2= -146 min., PS3 =-176 min). (*J*) Duration of cycle memory markedly increased when the effect of the light perturbation is decreased (*ptrbR* 0.006→0.002 in Eqn.13 and *ptrbS* 0.006→0.002 in Eqn. 14; PS1=PS2=PS3=0). Evidently cycle memory depends that light act as a small perturbation on a strongly rhythmic underlying limit cycle.

Next we reduced the rythmicity of the VIP feed back loop and this resulted in an immediate large phase shift when proceeding into constant darkness, which we interpreted as a loss of cycle memory (Fig. 9 *I*). We tested the opposite effect: reducing the effect of light on a strongly rhythmic VIP oscillation which markedly increased the duration of cycle memory (Fig. 9 *J*). Thus it appears that light-dark cycle memory and cycle-rate memory can be accounted for by a strongly rhythmic neuropeptide feed back loop upon which light acts as a perturbation. For memory what is important is that the light-perturbed VIP limit cycle be similar to the unperturbed cycle. Note that the SCN is about 100 times less sensitive to light than are the retina's rod cells (26). Note also that increasing the coupling strength between light and the SCN will increase range of entrainment and shorten acquisition time but that these come at the expense of cycle memory.

DISCUSSION

A strongly nonlinear negative feedback appears to be required in order to maintain the limit-cycle oscillation in the biochemistry inside an individual clock neuron (14). Leloup and Goldbeter noted that the strong rythmicity within a clock neuron's repressor feed back loop depended upon a strongly nonlinear negative feedback, characterized by a nonlinear feedback equation that used an exponent significantly greater than one (n = 4 in Eqns. 1 and 2). This choice made for a robust circadian oscillation of the clock proteins per and cry within a single uncoupled clock neuron in constant darkness. Apparently strong nonlinearities are also required in the coupling pathway between clock neurons in order to compete against and overcome the cell's own natural rhythm, so as to be able to synchronize clock neurons together in constant darkness. Strong nonlinearity within the neuropeptide feed back loop in the synch pathway between clock neurons permits for a high-contrast synchronizing signal to be exchanged between them, which then leads to a high degree of synchronization (exponents o in Eqn. 1 and p in Eqn. 11). Also, a strongly rhythmic VIP oscillation on which light acts only weakly leads functionally to light-dark cycle memory. This can be obtained by making the negative feed back within the loop strongly nonlinear (exponent p = 4 in Eqn. 11) and also by increasing loop gain ($c4$ in Eqn. 11, $c9$ in Eqn. 13a, $c11$ in Eqn 14a).

There is some controversy concerning the intrinsic rhythmicity of clock neurons, whether many remain rhythmic when uncoupled, and whether coupling should convey both synch and rhythmicity upon them (9, 34). Indeed, if a particular clock neuron has strong intrinsic rhythmicity with a period length that is several hours distinct from the

circadian day then it would seem that a very strong coupling would be required to synchronize it to the day. It's evident that a natural competition should arise between the intrinsic rhythmicity of an individual clock neuron and the rhythmicity of the loop that synchronizes them together. It's possible that many repressor and promoter feed back loops are intentionally made only weakly rhythmic in order to permit easier synchronization between them.

There is a natural question concerning the multiple actions of VIP: why should VIP act quickly to increase firing rate while at the same time inducing clock gene transcription and then later inhibit a clock neuron's own VIP production? Compare the VIP oscillation in the SCN in complete darkness with the voltage oscillation in a hair cell in the frog's hearing organ in complete quiet (41). In the quiet a current of potassium ions leaks into the hair cell, which depolarizes it and turns on a fast, voltage-gated calcium current that further depolarizes it (fast positive feed back). Calcium then binds with a time delay to a calcium-gated potassium channel which hyperpolarizes the cell (time-delayed negative feed back). When hyperpolarized all channels turn off and the leak current then restarts the cycle so that hair cell voltage sinusoidally oscillates by several millivolts in the quiet. Note that without the calcium current providing fast positive feed back the hair cell would not oscillate. Compare this to the neuropeptide oscillation in the SCN in constant darkness: as transmitted VIP increases, firing rate increases which then further increases transmitted VIP (fast positive feed back). Received VIP then inhibits VIP precursor with a time delay (time-delayed negative feedback). Similar to turning off the calcium current in the hair cell, if one reduces the VIP to firing rate gain then the VIP oscillation can be turned off. In both cases a fast

positive feed back followed by a slow negative one makes for spontaneous oscillation in the quiet or in the dark.

Day length on earth is almost exactly 24 hours with the only change being that hours of light are continually being traded for hours of darkness as we go from summer to winter, and vice versa. At 45 degrees north latitude our light-dark period changes from 16-8 in the summer to 9-15 in the winter with the fastest rate of decrease in light occurring near the fall equinox where the light period is shortening by about 4 minutes per day (40). What is the advantage to mammalian life on a rotating world that it be able to remember the light-dark cycle and the rate of change of this light-dark cycle? The SCN is in effect remembering the entraining signal by persisting with a long-lived transient limit cycle in its synchronized repressor feed back loops inside its coupled clock neurons. Here a comparison to electronics is useful: a 2nd order lock-in amplifier creates a replica signal at a slowly moving entraining frequency and thereby forms a memory for that entraining signal (42). Then its replica remains close to its locked frequency in the event of a signal dropout so that when the signal returns, reacquisition by lock-in or pull-in is very rapid. In a lock-in amplifier an active high-gain feed back loop is responsible for the long holding times. Also, note that a 3rd order lock-in has frequency rate memory together with frequency and phase memories. Thus it appears possible to make a reasonable comparison between the mammalian SCN with its high-gain VIP feed back loop and a high loop-gain lock-in amplifier. Here rapid signal reacquisition in case of a light-dark cycle dropout would seem to be one clear advantage. A second advantage for precisely remembering the location of the light and dark edges would likely be light-noise rejection, so that spurious or unexpected light or dark edges would result in

minimal phase-shifts. Here we note that the mammalian SCN has a type 1 PRC with a dead zone that rejects light-noise during the day, unlike simpler life forms with type 0 PRCs that lack a dead zone and thus permit light to phase shift the organism throughout the day (A). Investigations need to be made into the noise-rejection properties of a type 1 PRC with a dynamic dead zone.

We have shown that Siberian hamsters have several days of memory for a light-dark cycle. Cycle memory appears to be due to a strongly rhythmic VIP oscillation and that the dead zone in mammals can result from a strongly nonlinear kinase-phosphatase interaction. A good SCN is an extremely accurate timepiece that is correct to within several minutes out of the 1440 in a day (9). In the way that its clock neurons are intentionally kept in the dark and isolated away from spurious light, the way that their biochemical limit-cycles form a replica of a light-dark cycle and thus retain a memory of the entraining light-dark signal, the mammalian SCN resembles a lock-in amplifier (42).

REFERENCES

1. Moore-Ede, Martin C., Frank M. Sulzman, and Charles A. Fuller. 1982. The Clocks that Time Us. Harvard University Press, Cambridge, MA and London, UK.

2. Bretzel, H. 1903. *Botanische Forschungen des Alexanderzuges*. Leipzig: B. G. Teubner.

3. Goldbeter, Albert. 1996. Biochemical Oscillations and Cellular Rhythms: The Molecular Bases of Periodic and Chaotic Behavior. Cambridge University Press, Cambridge, UK.

4. Binkley, Sue. 1997. Biological Clocks: Your Owner's Manual. Harwood Academic Publishers, Amsterdam, The Netherlands.

5. Reppert, S. M. and D. R.Weaver. 2002. Coordination of circadian timing in mammals. Nature 418: 935–941.

6. Pittendrigh, C. S. and S. Daan. 1976b. A functional analysis of Circadian Pacemakers in Nocturnal Rodents. IV. Entraimnent: Pacemaker as Clock. *J. Comp. Physiol.* 106:291-331.

7. Kandel, Eric R., James H. Schwartz, and Thomas M. Jessell. 2000. Principles of Neural Science. 4th ed. McGraw-Hill, USA.

8. Welsh, D. K. ,D. E. Logothetis, M. Meister, and S. M. Reppert. 1995. Individual Neurons Dissociated from Rat Superchiasmatic Nucleus Express Independently Phased Circadian Firing Rythms. *Neuron* 14**:** 697-706.

9. Aton, S. J. and E. D. Herzog. 2005. Come Together, Right…Now: Synchronization of Rythms in a Mammalian Circadian Clock. *Neuron* 48:531-534.

10. Abrahamson, E. E. and R. Y. Moore. 2001. Suprachiasmatic nucleus in the mouse: retinal innervation, intrinsic organization and efferent projections. *Brain Res.* 916:172-191.

11. Dunlap, Jay C., Jennifer J. Loros, and Patricia J. Decoursey. 2004. Chronobiology: Biological Timekeeping. Sinauer Associates Inc., Sunderland, MA.

12. Ospeck, M., B. Coffey, and D. Freeman. 2009. Light-Dark Cycle Memory in the Mammalian Suprachiasmatic Nucleus. *Biophys J.* 6:1513-24

13. Yamaguchi S., H. Isejima, T. Matsuo, R. Okura, K. Yagita, M. Kobayashi, H. Okamura. 2003. Syncronization of cellular clocks in the suprachiasmatic nucleus. *Science* 302:1408-1412.

14. Leloup, J-C. and A. Goldbeter. 2003. Toward a detailed computational model for the mammalian circadian clock. *PNAS* 100:7051-7056.

15. Shinohara, K., K. Tominaga, Y. Isobe, S-I. T. Inouye. 1993. Photic Regulation of Peptides Located in the Ventrolateral Subdivision of the Suprachiasmatic Nucleus of the Rat: Daily Variations of Vasoactive Intestinal Polypeptide, Gastrin-releasing Peptide, and Neuropeptide Y. *J. Neurosci.* 13(2):793-800.

16. Itri, J., C. S. Colwell. 2003. Regulation of Inhibitory Synaptic Transmission by Vasoactive Intestinal Peptide (VIP) in the Mouse Suprachiasmatic Nucleus. *J. Neurophysiol.* 90:1589-1597.

17. Pakhotin, P., A. J. Harmar, A. Verkhratsky, H. Piggins. 2006. VIP receptors control excitability of suprachiasmatic nuclei neurons. *Eur. J. Physiol.* 452:7-15.

18. Pennartz, C. M. A., M. T. G. De Jeu, N. P. A. Bos. J. Schaap, A. M.S. Geurtsen. 2002. Diurnal modulation of pacemaker potentials and calcium current in the mammalian circadian clock. *Nature* 416:286-290.

19. Ikeda, M., T. Sugiyama, C. S. Wallace, H. S. Gompf, T. Yoshioka, A. Miyawaki, C. N. Allen. 2003. Circadian dynamics of cytosolic and nuclear Ca^{2+} in single suprachiasmatic nucleus neurons. *Neuron* 38:253-263.

20. Zylka, M. J., L. P. Shearman, D. R. Weaver, S. M. Reppert. 1998. Three period Homologs in Mammals: Differential Light Responses in the Suprachiasmatic Circadian Clock and Oscillating Transcripts Outside of the Brain. *Neuron* 20:1103-1110.

21. Vosko, A. M., A. Schroeder, D. H. Loh, and C. S. Colwell. 2007. Vasoactive intestinal peptide and the mammalian circadian system. *Gen Comp Endocrinol*. 152(2-3):165-175.

22. Moore, Robert Y. 1999. Circadian Timing. chp. 45 in Fundamental Neuroscience. Ed. Michael J. Zigmond, Floyd E. Bloom, Story C. Landis, James L. Roberts, Larry R. Squire. Academic Press, San Diego, CA.

23. Pizzio, G. A., E. C. Hainich, G. A. Ferreyra, O. A. Coso, D. A. Golombek. 2003. Circadian and photic regulation of ERK, JNK and p38 in the hamster SCN. *Neuroreport* 14(11):1417-1419.

24. Doi, M., S. Cho, I. Yujnovsky, J. Hirayama, N. Cermakian, A.C. B. Cato, P. Sassone-Corsi. 2007. Light-Inducible and Clock-Controlled Expression of MAP Kinase Phosphatase 1 in Mouse Central Pacemakere Neurons. *Journal of Biological Rhythms* 22(2):127-139.

25. Meijer, J. H., K. Watanabe, J. Schaap, H. Albus, L. Detari. 1998. Light Responsiveness of the Suprachiasmatic Nucleus: Long-Term Multiunit and Single-Unit Recordings in Freely Moving Rats. *J. Neurosci.* 18(21): 9078-9087.

26. Nakamura, T. J., K. Fujimura, S. Ebihara, K. Shinohara. 2004. Light response of the neuronal firing activity in the suprachiasmatic nucleus of mice. *Neurosci. Letters* 371:244-248.

27. Maywood E., J. O'Neill, J. E. Chesham, and M. H. Hastings. 2007. Minireview: The Circadian Clockwork of the Suprachiasmatic Nuclei---Analysis of a Cellular Oscillator that Drives Endocrine Rhythms. *Endocrinology* 148(12):5624-5634.

28. Travnickova-Bendova, Z., N. Cermakian. S. M. Reppert, P. Sassone-Corsi. 2002. Bimodal regulation of mPeriod promoters by CREB-dependent signaling and CLOCK/BMAL1 activity. *PNAS* 99(11):7728-7733.

29. Strogatz, S. 1994. Nonlinear Dynamics and Chaos. Perseus Books, Reading, MA.

30. Buck, J. 1988. Synchronous rhythmic flashing of fire flies, part II. *Q. Rev. Biol*. 63(3):265-289.

31. Strogatz, S. 2003. Sync: How Order Emerges from Chaos in the Universe, Nature, and Daily Life. Hyperion Press.

32. Gonze, D., S. Bernard, C. Waltermann, A. Kramer, and H. Herzel. 2005. Spontaneous Synchronization of Coupled Circadian Oscillators. *Biophysical Journal* 89:120-129.

33. Bernard, S., D. Gonze, B. Cajavec , H. Herzel and A. Kramer. 2007. Synchronizationinduced rythmicity of circadian oscillators in the superchiasmatic nucleus. *PLOS Comp. Bio.* 3(4):0667-0679.

34. To, T-L., M. A. Hensen, E. D. Herzog, F. J. Doyle III. 2007. A Molecular Model for Intercellular Synchronization in the Mammalian Circadian Clock. *Biophysical J.* 92:3792-3803.

35. Puchalski, W. and G. R. Lynch. 1992. Relationship between Phase Resetting and the Free-Running Period in Djungarian Hamsters. *Journal of Biological Rhythms* 7(1):75-83.

36. Colwell, C. S., S. Michel, J. Itri, W. Rodriguez, J. Tam, V. Lelievre, Z. Hu, J. A. Waschek. 2004. Selective deficits in the circadian light response in mice lacking PACAP. *Am. J. Physiol.* 287:R1194-R1201.

37. Leloup, J-C. and A. Goldbeter. 1998. A Model for Circadian Rythms in Drosophila Incorporating the Formation of a Complex between the PER and TIM proteins. *Journal of Biological Rhythms* 13 :70-87.

38. Theodosiou, A., A. Ashworth. 2002. Protein family review MAP kinase phosphatases. *Genome Biology* 3(7) reviews3009.1-3009.10.

39. Garcia-Ojalvo, J., M.B. Elowitz, and S. H. Strogatz. 2004. Modeling a synthetic multicellular clock: repressilators coupled by quorum sensing. *PNAS* 101:10955-10960.

40. Shing Lam compiled the C code based on a formula published in: Meeus, Jean . 1991. Astronomical algorithms. Richmond, Va.: Willmann-Bell. ISBN 0943396352

41. Ospeck, M., V. M. Egu`iluz, and M. O. Magnasco. 2001. Evidence of a Hopf bifurcation in frog hair cells. *Biophysical Journal* 80: 2597-2607.

42. Gardner, F. M. 1979. Phaselock Techniques. 2nd ed. John Wiley and Sons NY, NY.

APPENDIX

Biophysical Journal Volume 97 September 2009 1513–1524

Light-Dark Cycle Memory in the Mammalian Suprachiasmatic Nucleus

Mark C. Ospeck,[†*] Ben Coffey,[†] and Dave Freeman[‡]
[†]Physics Department and [‡]Biology Department, University of Memphis, Memphis, Tennessee

ABSTRACT The mammalian circadian oscillator, or suprachiasmatic nucleus (SCN), contains several thousand clock neurons in its ventrolateral division, many of which are spontaneous oscillators with period lengths that range from 22 to 28 h. In complete darkness, this network synchronizes through the exchange of action potentials that release vasoactive intestinal polypeptide, striking a compromise, free-running period close to 24 h long. We entrained Siberian hamsters to various light-dark cycles and then tracked their activity into constant darkness to show that they retain a memory of the previous light-dark cycle before returning to their own free-running period. Employing Leloup-Goldbeter mammalian clock neurons we model the ventrolateral SCN network and show that light acting weakly upon a strongly rhythmic vasoactive intestinal polypeptide oscillation can explain the observed light-dark cycle memory. In addition, light is known to initiate a mitogen-activated protein kinase signaling cascade that induces transcription of both *per* and *mkp1* phosphatase. We show that the ensuing phosphatase-kinase interaction can account for the dead zone in the mammalian phase response curve and hypothesize that the SCN behaves like a lock-in amplifier to entrain to the light edges of the circadian day.

INTRODUCTION

Mammals have two suprachiasmatic nuclei (SCN), one per hemisphere, located in the hypothalamus just above the optic chiasm. These two neural networks constitute the mammalian circadian clock, the master clock responsible for driving circadian locomotor activity rhythms and synchronizing these rhythms to the 24-h day. Within the SCN, clock neurons are synaptically coupled so that they synchronize their biochemical limit cycles together in complete darkness (1,2,3). Mammals exhibit multiple circadian rhythms in physiology and behavior that persist in constant conditions and exhibit a coherent period length in the absence of external time cues (4), with the SCN being the principal coordinator of these rhythms (5).

Rhythmic activity of SCN neurons is thought to be driven by the rhythmic expression of so-called clock genes (*per*1, *per*2, *per*3, *cry*1, *cry*2, *bmal*1, and *reverbα*) and individual neurons exhibit circadian rhythms in electrical activity and gene expression in vitro that have independent period lengths and phases (6). However, for synchronization to occur between clock neurons, intercellular interaction appears to be necessary, because SCN neurons placed at low densities in culture exhibit rhythmic activity, but fail to synchronize together (6). Also, exposing SCN neurons to tetrodotoxin in vitro causes desynchronization, which suggests that synaptic communication is involved in their synchronization (3,7). In support of this hypothesis, synchrony is observed in SCN slices or SCN neurons kept in vitro at high densities, which presumably allows synaptic communication between them (3,7).

Neuropeptides, including vasoactive intestinal polypeptide (VIP (3,8)) and gastrin-releasing peptide (9), together with the neurotransmitter gamma aminobutyric acid (GABA (10)), have been considered as synchronization factors in the SCN. Recent results support an integral role for VIP in both intracellular timekeeping and intercellular synchrony among SCN neurons (3,8,11). Synchrony among neurons is lost in knockout mice lacking VIP ($VIP^{-/-}$) or its receptor $VPAC_2$, which is a product of the *Vipr*2 gene (8). Treatment of $VIP^{-/-}$ mice with a $VPAC_2$ agonist restored rhythmicity and synchrony in cultured SCN neurons (8). Also, exposure to exogenous VIP resulted in phase shifts of individual SCN neurons, as well as phase shifts at the behavioral level (12,13). Increases in $VPAC_2$ receptor number caused more rapid reentrainment to phase shifts of the light-dark cycle in mice and desynchronized their rhythms in constant darkness (14). In addition, mice that lacked the $VPAC_2$ receptor exhibited arrhythmic activity in constant darkness (15). Both VIP and the $VPAC_2$ receptor appear to be essential for circadian function in the mouse SCN (15).

The neurotransmitter GABA exhibits a circadian rhythm of release in the SCN (16) and exogenously applied GABA phase-shifts the neuronal firing rate of SCN neurons in vitro, whereas daily administration of GABA synchronizes this rhythm (10). Ionotropic $GABA_A$, as well as the G-protein-coupled $GABA_B$ receptors, is expressed within the SCN (3), and there is evidence that GABA contributes to synchrony, although in a less direct way than does VIP (17).

Previous models of the SCN investigated its synchronization through the nonuniform oscillator equation (18), via synthetic genetic circuits called repressilators (19), by using gate cells to couple van der Pol oscillators together (20), and by a mean field coupling of the neuropeptide VIP between biophysics-based models of clock neurons (21–23). Meanwhile, individual mammalian clock neuron biochemistry has been extensively modeled (24,25–27), along with a detailed model of VIP activating the $VPAC_2$ receptor,

Submitted December 23, 2008, and accepted for publication June 8, 2009.

*Correspondence: mospeck@memphis.edu

Editor: Arthur Sherman.

0006-3495/09/09/1513/12 $2.00

doi: 10.1016/j.bpj.2009.06.010

causing activation of a cyclic adenosine monophosphate (cAMP)/protein kinase A (PKA) intercellular signaling pathway (28). Recently, there has been a great deal of interest in biophysics-based models over qualitative modeling (29) and also in heterogeneous modeling of the SCN (30).

We show experimentally that the Siberian hamster (*Phodopus sungorus*), a nocturnal mammal, forms a memory for the particular light-dark cycle to which it was entrained. We then use Leloup-Goldbeter model mammalian clock neurons (24) to make a biophysics-based model of the ventrolateral (VL) subdivision of the SCN to try to account for the light-dark cycle memory we observe.

METHODS

Animals were cared for in accordance with the University of Memphis Institutional Animal Care and Use Committee. Siberian hamsters were placed one per cage, each with a running wheel wired to make one spike per wheel revolution. Running wheel "actograms" were then acquired by Clocklab data analysis and collection software (Coulbourn Instruments, Allentown, PA), which ran on a PC running a Windows XP operating system. Activity was continuously recorded first with the animals placed on various light-dark schedules for a number of weeks and afterward with the animals in constant darkness for several weeks. We employed light-dark schedules that usually involved phase-advancing the lights-off time by 5–20 min/day. Clocklab software was used to turn on and off two 11-W incandescent bulbs. For certain static light-dark schedules such as 10–14 light-dark fluorescent room lights were used. The four fluorescent lights were expected to provide ~11,000 Lumens of flux and actually gave ~2000 candles/m^2 when measured by using a spot meter at the animal cages, similar to the incandescent lamps. Actograms were then analyzed using Clocklab software, which made linear fits to the onset of running wheel activity. These fits were used to determine the circadian period of the animal when it was entrained to a given cycle and the circadian period for the first several days in the constant darkness that followed a particular light-dark cycle. Also, we obtained the animal's free-running period by making fits after the animal had spent several weeks in constant darkness.

EXPERIMENTAL RESULTS

A series of running-wheel activity experiments were performed on Siberian hamsters to study the memory they would retain of a particular light-dark cycle when the cycle was immediately followed by a period of constant darkness. Fig. 1, *A–D*, shows actograms for animals that were entrained to static 10–14, 14–10, 11–11, and 13–13 light-dark cycles. Animals were first entrained to a particular light-dark cycle, and this was followed by constant darkness. A linear best fit to the animal's onset of activity was made when it was entrained to the cycle and also for the next several days in constant darkness. To quantify the number of days of cycle memory, we examined the standard deviation for the best fit to activity onset as a function of the number of days in constant darkness. Animals entrained to cycles with a 24-h period length usually persisted with several days of memory for that cycle ($n = 22$, average cycle memory $= 2.0 \pm 0.3$ days). We performed a p-test using the null hypothesis that these animals had no memory, obtaining $p \sim 10^{-7}$, which led us to conclude that Siberian hamsters retain a significant amount of memory for a light-dark cycle whose period length was close to 24 h. We note that the average free-running period for 31 animals was 23.8 ± 0.4 h. Next, we tested a second group of animals on light-dark cycles either longer or shorter than 24 h by a couple of hours (11–11 h, and 13–13 h). Here, the animals retained on average <1 day of memory ($n = 9$, average cycle memory $= 0.8 \pm 0.15$ days, $p \sim 0.0004$ for no-memory null hypothesis). Thus, the second group also showed a small amount of memory. We also did a preliminary range of entrainment experiments on a small number of Siberian hamsters and found that 2 of 4 animals were able to entrain to a 10-10 cycle, 3 of 12 were able to entrain to an 11-11 cycle, and 6 of 12 were able to entrain to a 13-13 cycle, but 0 of 4 were able to entrain to a 14-14 cycle. Twenty-six results were discarded, due in almost all cases to the animal's failure to properly entrain to the light schedule. Fig. 1, *E–H*, shows that a nocturnal mammal also clearly retains several days of memory for the position of a slowly moving light-dark edge. Typically, we would start the animals on a 16-8 cycle and then phase-advance their lights-off time by 5–20 min/day, trading hours of light for hours of darkness while maintaining a 24-h period. We intended that these changes would mimic the changes in day length occurring at high latitudes near an equinox.

Evidently, Siberian hamsters are able to form a short-term memory of the particular light-dark cycle to which they are entrained and are also able to anticipate slowly changing light-dark cycles. We chose to focus on the light-dark edge and activity onset because nocturnal animals normally start their activity at lights-off and light is thought to be the primary zeitgeiber, or time giver, in the SCN (1,2). Since synaptic input from the retina is made to the VL part of the SCN, which is thought to be principally responsible for synchronization of the entire organ (3,7,31), in modeling it, we try to account for synchronization and light-dark cycle memory.

Model

Different regions of the SCN employ different neuropeptide transmitters, and there is evidence that these regions are distinct oscillators (32). Action potentials from neurons in the VL part of the SCN transmit VIP. Leloup and Goldbeter (LG) (24) have constructed a low-dimensional model of a mammalian clock neuron, and we couple these neurons via action potentials that exchange VIP to model the VL SCN. The LG model neuron contains three circadian biochemical feedback loops. Its repressor loop uses the clock proteins PER and CRY in an ~12-h negative feedback loop in which *per* and *cry* RNAs are first transcribed and then translated into proteins that dimerize (Fig. 2 *A*). Subsequently, PER-CRY protein dimers enter the nucleus to repress both *per* and *cry* RNA transcription by binding to the CLOCK-BMAL1 dimers that promote such transcription. Note that a 12-h negative feedback loop means that

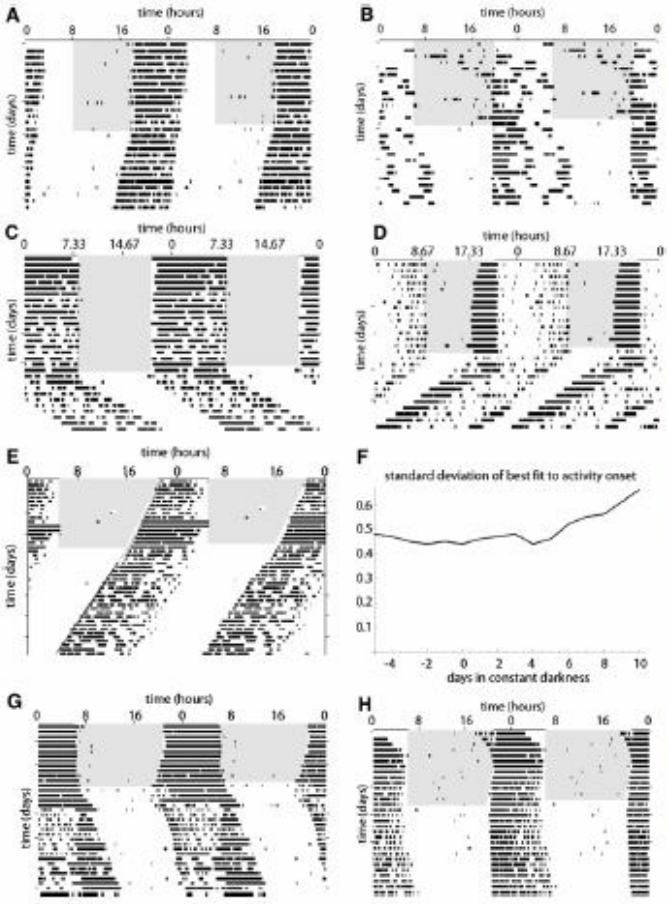

FIGURE 1 Siberian hamsters form a memory for the particular light-dark cycle to which they are entrained. Shown are running-wheel actograms for these nocturnal mammals, whose activity normally starts at lights off. The actogram is repeated with pairs of days plotted side by side. Black bars indicate running-wheel activity; the gray region shows the duration of the light period as the day number increases from top to bottom. The animal is first entrained to a particular cycle, which is followed by constant darkness. Linear least-square fits to activity onset are used to quantify the number of days of memory an animal retains for a particular cycle. (*A*) Entrainment to a 10-14 light-dark cycle followed by ~2 days of memory. (*B*) Entrainment to a 14-10 cycle followed by ~2 days of memory. (*C*) Entrainment to an 11-11 cycle followed by 1 day of memory. (*D*) Entrainment to a 13-13 cycle followed by 1 day of memory. Note here that activity onset precedes the light-dark edge by a large phase angle. Siberian hamsters also form a memory for the rate of change of a particular light-dark cycle to which they are entrained. Two fits are shown: first, a linear fit to the animal's onset of activity when it is entrained to the cycle and for the next several days in constant darkness; and, well into constant darkness, a fit made to determine the animal's FRP. (*E*) Animal with a short FRP (23.58 h) starts on a 16-8 cycle where lights-off is phase-advanced by 20 min/day for 15 days. Afterward, in constant darkness, the animal retains ~4 days of memory for the phase-advancing dark edge. (*F*) Standard deviation for the best fit to activity onset in *E* begins to increase after ~5 days in constant darkness are included in the fit. (*G*) An animal with a long (24.19-h) FRP retains ~3 days of memory for the phase-advancing light-dark cycle, from a 16-8 cycle where lights-off was phase-advanced by 15 min/day for 7 days. (*H*) Animal with a 24.05-h FRP is started on a 16-8 cycle where lights-off is phase-advanced by 10 min/day for 7 days. The animal retains ~2 days of memory for this phase-advancing cycle.

input of a pulse of *per* RNA results in a negative response in *per* RNA in 12 h. A second promoter feedback loop is also an ~12-h negative feedback loop in which nuclear BMAL1 represses its own transcription. Also, there is a REVERBα negative feedback loop in which CLOCK-BMAL1 induces *reverbα* transcription, with REVERBα protein later relocating to the nucleus to repress *bmal1* transcription. This REVERBα loop is one of several interesting lithium-sensitive components of the clock (33–35); however, it is not part of the LG basic model, so to keep things as simple as possible we do not include it here.

However, there is clear experimental evidence that constant light lowers the content of VIP within the SCN, exponentially damping it with an ~8-h time constant (36). Consistent with this, the VIP content of the SCN oscillates in a circadian fashion when locked to a 12-12 light-dark cycle and exhibits a smaller, but similar, oscillation in constant darkness (36). During daylight or subjective day, when firing rate and VIP exchange is high, SCN VIP content continues to decrease. This leads us to include a third ~12-h negative feedback loop in which the VIP received by a clock neuron slowly damps that neuron's own VIP production. The neuropeptide VIP is a rhythmically expressed clock protein that meets most of the criteria for being a synchronizing factor (3), and neuropeptides are transcribed so that they offer a natural mechanism for coupling between biochemistry and electrical firing activity within a network of neurons. VIP has many effects. Specifically, it is known to induce transcription of *per* (37) and *mkp1* (38), a phosphatase for MAP kinase. In addition, it depolarizes a clock neuron by ~12 mV and initiates a subthreshold membrane potential oscillation, both of which act to increase firing rate (16, 40–42).

Expression of the clock gene *per* is induced by light. In constant darkness, *per* RNA is known to peak around time circadian time 8 during the subjective day while 15-min light pulses act to sharply increase *per* RNA levels within ~1 h (37). Light striking retinal ganglion cells causes cotransmission of both pituitary-adenylate-cyclase-activating polypeptide (PACAP) and glutamate along axons of the retinohypothalamic

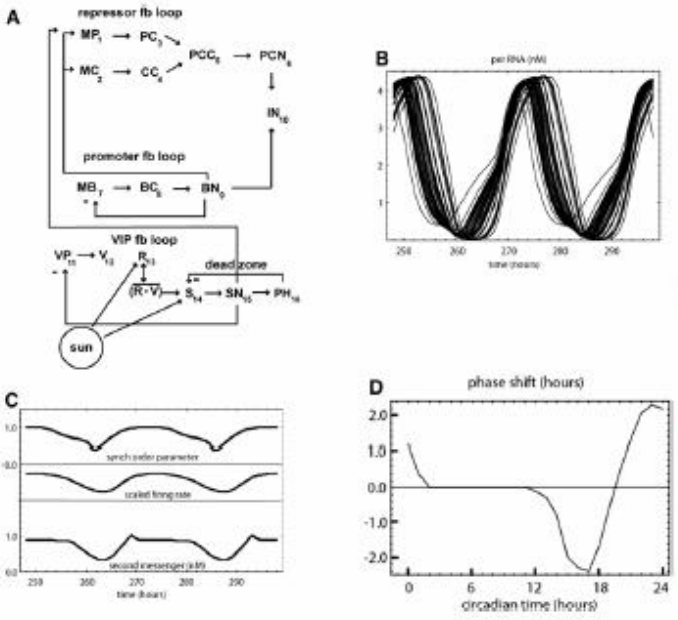

FIGURE 2 (*A*) Sixteen dynamical variables and four feedback loops represent each clock neuron. Indices show the corresponding equation number in the Appendix. In constant darkness, an oscillation in the neuropeptide VIP (V) drives oscillations in the firing rate (R), which peaks near CT7, and in the second messenger (S), which causes *per* RNA (MP) to peak near CT8, synchronizing the network (37,44). All feedback loops are internal within a single clock neuron, except that in the VIP loop it is the average rate of receiving VIP from other clock neurons ($\overline{R \times V}$) that sets the target firing rate and second messenger. Light acts in this loop to increase the firing rate and second messenger, causing induction of *per* RNA within ~1 h (37). The dead zone, where the network is insensitive to phase-shifting by light, can be accounted for by a strongly nonlinear phosphatase-kinase (PH-S) interaction. (*B*) *per* RNA shown for 50 clock neurons whose repressor and promoter feedback loops synchronize together in constant darkness through the exchange of VIP. Neurons are given a Gaussian distribution in the period lengths of their repressor and promoter feedback loops, with an average period of 24.0 h and a standard deviation of 1.2 h. (*C*) *Upper*: Synchronization order parameter, $synch = \frac{\text{variance}_{\text{pop}}\,[\text{mean}_{\text{cell}}\,(MP_i)]}{\text{mean}_{\text{cell}}\,[\text{variance}_{\text{pop}}\,(MP_i)]}$, where 1.0 is perfect synchronization and 0.0 is no synchronization (19,21). *Middle*: Scaled firing rate, R, which oscillates by an factor of ~2. *Lower*: Second-messenger MAPK S. (*D*) Phase response curve constructed by measuring the model network's phase shift due to a 15-min pulse of light in constant darkness (light pulse represented by $ptrbR = 0.04$ in Eq. A13 and $ptrbS = 0.08$ in Eq. A14).

tract, which terminates in the VL part of the SCN (2), where they increase the average firing rate, which in turn increases the rate at which VIP is transmitted between clock neurons. Both PACAP and VIP are known to bind to the $VPAC_2$ receptor, from which they initiate cAMP/PKA, Ca^{2+}, and MAP kinase signaling pathways that lead to the phosphorylation of cAMP response element binding protein (CREB), which in turn leads to the induction of *per* (38,43,44). However, it has been found recently that acute light-dependent increase of *per* RNA in mouse can result via an *n*-methyl-*d*-aspartate (NMDA) receptor pathway that is independent of VIP (45), so it appears that *per* transcription can be activated by both the VIP and NMDA pathways. Part of the mechanism involves a kinase being translocated to the nucleus, where it turns on CREB, a nuclear transcription factor that binds to a specific sequence of DNA to upregulate clock gene transcription. In the nucleus, phosphorylated CREB acts independently of the CLOCK-BMAL1 promoter to induce both *per* and *mkp1* transcription (46), so we assume that the VIP/NMDA → MAPK → CREB and CLOCK-BMAL1 pathways act in parallel to promote *per* transcription. It would seem that VIP is forcing a *per* oscillation in constant darkness and light-induced *per* is phase-shifting the oscillation.

Clock neurons are unusual in that they spike only slowly in the 1- to 10-Hz range. Their average firing rate oscillates in constant darkness, increasing by a factor of ~2 during subjective day, with their peak firing rate occurring around circadian time 7 (47), ~1 h before the peak in *per* RNA (37). Together, these findings lend support to the hypothesis that in constant darkness, an oscillation in the VIP should be able to drive both firing rate and *per* transcription so as to synchronize the network. Also, the hyperpolarizing neurotransmitter GABA is cotransmitted along with depolarizing VIP, and SCN neurons are ~3 times more likely to increase their firing rate during subjective night, when GABA cotransmission is lower, as compared with subjective day (48). We assume that one purpose of GABA cotransmission is to limit the increase in firing rate when a clock neuron receives VIP, so that during subjective day, when GABA exchange is relatively high, it causes the firing rate to saturate.

Central to the LG mammalian clock neuron model is the neuron's repressor feedback loop, where *per* and *cry* RNAs (MP and MC) are transcribed, translated into clock proteins (PC and CC), and then dimerized (PCC). As dimers they enter the nucleus to form a repressor that binds to CLOCK-BMAL1 promoter (PCN and BN dimerize to make IN), thus inhibiting the transcription of *per* and *cry* RNA (24). Our model neuron's first 10 dimensions describe its repressor and promoter feedback loops and are taken directly from the LG model, from which we have omitted six phosphorylation-degradation pathways. We add six dimensions involving firing rate and VIP exchange between neurons so that each neuron is described by 16 variables shown in Fig. 2 *A*. Our model is a network of such neurons, each accounted for by 16 first-order differential equations, one each for the time rate of change of a neuron's *per*

RNA$\frac{d[MP]}{dt}$, *cry* RNA$\frac{d[MC]}{dt}$, etc. Below is a list of the variables, together with their interrelationships, that are accounted for by the time evolution of differential equations in the Appendix.

Repressor feedback loop:

1. *MP* = *per* RNA transcription activated by CLOCK-BMAL1 (*BN*), which is inhibited by nuclear PER-CRY dimer (*PCN*). This transcription is independently activated by phosphorylated CREB (*SN*).
2. *MC* = *cry* RNA transcription activated by CLOCK-BMAL1 (*BN*).
3. *PC* = PER protein translated from *per* RNA (*MP*).
4. *CC* = CRY protein translated from *cry* RNA (*MC*).
5. *PCC* = PER-CRY dimer made from *PC* and *CC*.
6. *PCN* = PER-CRY dimer in the nucleus, which binds CLOCK-BMAL1 (*BN*), repressing transcription of *per* and *cry*.

Promoter feedback loop:

7. *MB* = *bmal1* RNA, inhibited by nuclear BMAL1 (*BN*) protein. *clock* is transcribed at a constant rate so that its protein is considered an implicit part of BMAL1 (24).
8. *BC* = BMAL1 protein translated from *bmal1* RNA.
9. *BN* = nuclear BMAL1 protein, which inhibits *MB* and activates *per* and *cry* transcription.

Repressor loop couples to promoter loop:

10. *IN* = inhibitor of *per* and *cry* transcription. Inhibitor is made when PER-CRY (*PCN*) dimerizes to CLOCK-BMAL1 (*BN*), preventing it from activating *per* and *cry* transcription.

Negative feedback loop, in which received VIP damps a clock neuron's own VIP production:

11. *VP* = VIP precursor, inhibited by received VIP, presumably via nuclear CREB (*SN*).
12. *V* = VIP neuropeptide, made by VIP precursor and exchanged between clock neurons.
13. *R* = clock neuron firing rate.
14. *S* = MAP kinase phosphorylated due to VIP binding to the $VPAC_2$ receptor, as well as by NMDA receptors activated by afferents from ganglion cells exposed to light (45).
15. *SN* = nuclear CREB turned on by MAP kinase, which then induces *per* (*MP*) and *mkp1* (*PH*) transcription. We assume that *SN* damps VIP precursor (*VP*).
16. *PH* = MKP1 phosphatase whose RNA is induced by CREB (*SN*). *PH* dephosphorylates/shuts off the MAP kinase signal (*S*).

The repressor loop spontaneously oscillates in a limit cycle that depends on the strongly nonlinear feedback to RNA transcription provided by *BN* (see Appendix, Eqs. A1–A6). The promoter loop (*MB*, *BC*, and *BN* in Eqs. A7–A9) also oscillates, but this oscillation depends upon a weaker nonlinearity for its negative feedback than does the repressor loop and so has a smaller exponent—$m = 2$ in Eq. A7 versus $n = 4$ in Eqs. A1 and A2—and is less rhythmic than the repressor loop (24).

In constant darkness, the SCN is able to compromise on a free-running period (FRP) that varies from animal to animal but is usually within a half-hour of 24 h long (1,2). However, single neurons within the SCN have a wide variance in the natural period of their repressor and promoter feedback loops, with period lengths that range between 22 and 28 h (1). To obtain a distribution of natural periods within the network, we used a Gaussian-distributed random variable, s_i, as a scale factor that multiplied all the rate constants for the repressor and promoter feedback loops inside a given neuron ($s_i = 1.0 \pm 0.05$ standard deviation in Eqs. A1–A10) We did not include such rate-constant noise in the VIP feedback loop, although small amounts of it produced similar results (include scale factor with 0.02 standard deviation in Eqs. A11–A16). Also, although the VL SCN includes several thousand neurons, we were only able to simulate all-to-all coupling between 50 neurons for times <1000 h on a PC. Simulations were run using Mathematica 5.2 on a Dell computer with a Microsoft Windows XP operating system and an Intel Pentium 4 processor (model in support file). We construct a basic model in which light causes a fast increase in second messenger (*S*), which induces both *per* and phosphatase transcription. Induced *per* phase-shifts the repressor feedback loops inside the clock neurons, whereas high levels of phosphatase block further second-messenger signal and establish a dead zone in which the clock neurons become insensitive to phase-shifting by light.

SIMULATION RESULTS

A network of LG model clock neurons can be coupled together through the exchange of the neuropeptide VIP. When VIP is made to oscillate in a 12-h negative feedback loop (*VP*, *V*, *R*, *S*, *SN*; Eqs. A11–A15) received VIP causes fast *per* transcription, which synchronizes all the repressor loops together in constant darkness (Eq. 1 and Fig. 2 *B*). This synchronization depended on several factors: first, that the received neuropeptide would quickly increase firing rate together with *per* transcription; second, that the received neuropeptide would slowly couple back to inhibit the neuropeptide precursor; and third, that this feedback loop would be strongly rhythmic. Strong rhythmicity in turn depended on the received VIP inhibiting a clock neuron's own VIP production through a high-gain, nonlinear negative feedback (Eq. A11).

Electrically we consider a clock neuron as a small capacitor with a voltage threshold that, when surpassed, results in an action potential. A VIP received from other clock neurons increases membrane potential and firing rate, whereas a received GABA has the opposite effect, decreasing membrane potential and firing rate. Firing rate is also increased by positive leak conductance turned on by retinal ganglion cells that are exposed to light. Thus, our target

firing rate is proportional to the product of the average firing rate and the VIP $\overline{(R \times V)}$ when this product is small, but then saturates due to the cotransmission of GABA when this product becomes large. In addition, the target firing rate includes a step function representing input from retinal ganglion cells that are exposed to light (Eqs. A13 and A13a).

We obtained a phase-response curve (PRC) for the synchronized network where a pulse of light was represented by two step functions that immediately increased the rates of change of both the firing rate and the second messenger. Then, by adjusting the strength of these light-induced increases in $\dot{R}$ and $\dot{S}$, the recorded phase shifts due to 15-min light pulses could be made similar to PRCs obtained from mammalian experiments (2,52) (Fig. 2 *D*). Physically, light causes the transmission of glutamate and PACAP along axons of the retino hypothalamic tract to the VL SCN, so it is logical that the light-induced second messenger (S) exists in part due to PACAP binding to the $VPAC_2$ receptor (53). Also, it is now known that acute light-dependent increase of *per* RNA in mouse can result via an NMDA receptor pathway that is independent of VIP and the $VPAC_2$ receptor (45). Meanwhile, VIP (V) is being continuously exchanged between clock neurons, so our second-messenger target was proportional to the product of the average firing rate and the VIP $\overline{(R \times V)}$ plus a step that we attribute to light-induced input from retinal ganglion cells (Eqs. A14 and A14a). Light-induced increases in firing rate also act to increase S.

The generic PRC includes an interesting region ~9 h long called the dead zone, where the mammal is insensitive to phase-shifting by light (2). Unlike the mammal, fruit fly clock neurons see the light, which acts directly through chromophores within them to degrade clock proteins and induce phase shifts (54). Clock protein concentration oscillates so that when it is low, the fly becomes insensitive to phase shifting by light. However, it appears that phase-shifting and dead zone in mammals work by a different principle, since mammalian clock neurons are kept from seeing sunlight directly and their clock proteins are known to peak during the late part of the dead zone. In the mammal, instead of degrading clock proteins, light induces transcription of both *per* and *mkp1* phosphatase (37,38). It is interesting that light uses cAMP/PKA, Ca^{2+}, and MAP kinase signaling pathways for this gene induction and that one of the induction targets is a phosphatase that dephosphorylates MAP kinase. This interaction between kinase and phosphatase is known to be very strongly nonlinear, and we hypothesize that it is responsible for the dead zone ((55); exponent $q = 50$ step function in Eq. 14b). Light causes an increase in phosphorylated kinase signal, which is followed by the induction of dephosphorylated phosphatase. Kinase phosphorylates the phosphatase, changing its conformation so that it will dephosphorylate a future kinase signal (55). Thus, whenever the kinase-phosphatase product exceeds a certain threshold, it will establish a dead zone. This interaction acts to truncate the phosphorylated kinase signal (Fig. 2 *C*), and effectively would make the SCN into a light-edge detector.

In constant darkness, our simulated dead zone is generic and ~9 h long (2). Note that there is experimental evidence that the width of the Siberian hamster's dead zone shortens to ~7 h after the animal has been entrained to a winter 9-15 light-dark cycle (52), the implication being that cycle memory makes the dead zone into a dynamic rather than a static interval. We note that in our simulations, the dead zone expands to ~12 h after entrainment to a summer 16-8 light-dark cycle. However, our simulated dead zone does not shorten after entrainment to a winter 8-16 cycle, but would do so if short day lengths were to downregulate VIP to second-messenger signaling $\overline{(R \times V)} \rightarrow S$. Also, there is recent experimental evidence that something like a kinase-phosphatase mechanism is responsible for the dead zone. Without $VPAC_2$ signaling, the mouse SCN becomes inappropriately responsive to phase shifting by light during the day, the implication being that VIP signaling is responsible for the dead zone, as shown by Maywood et al. (45). In that experiment, light via an NMDA pathway was able to acutely induce *per* during the supposed dead zone for the $Vipr2^{-/-}$ mutant mouse whose *mPer1* RNA (and presumably also *mkp1* RNA) remained low throughout the circadian day. In our model, it is VIP-driven *mkp1* induction that is responsible for the dead zone.

We tested the model's ability to entrain to the circadian day by using step functions to make sequences of light periods. The network had a free-running period of 24.0 h and was able to phase shift by 10–12 h in 6–7 days, advancing or delaying to acquire lock to a 12-12 light-dark cycle (Fig. 3). Increasing or decreasing the coupling strength between light and the network respectively decreased or increased the time to acquire the cycle. The coupling strengths, $ptrbR = 0.006$ in Eq. A13 and $ptrbS = 0.006$ in Eq. A14, were chosen to be consistent with time-to-entrain, cycle-memory, and limits-of-entrainment experiments ((1); see Fig. 1 *B*).

We next investigated the model's memory for the particular light-dark cycle to which it was entrained, together with its limits of entrainment. Fireflies are known to have a resetting strength where a larger strength permits synchronization between two flies with more dissimilar frequencies (49–51). Here, the coupling is between a network with a 24.0-h free-running period and a specific light-dark cycle. Our light periods are defined by the height of the step changes they make in $\dot{R}$ and $\dot{S}$ ($ptrbR = 0.006$ in Eq. A13 and $ptrbS = 0.006$ in Eq. A14). This choice permitted the network to entrain cycle lengths between ~22 and 26 h, whereas our experimental range of entrainment was 20–26 h (Fig. 4, *A*, *B*, *E*, and *F*). Holding day length constant, we locked the network to various light-dark cycles. When fixed to a 24-h day length, the model was able to remember the particular cycle, i.e., 10-14, 14-10, etc. that it was locked to as it proceeded into constant darkness (Fig. 4, *C* and *D*). Cycle-rate memory tests began with 12-12 light-dark cycles, which for 12 days increased or decreased their light period by 10 min per day to mimic large day-length changes that occur at

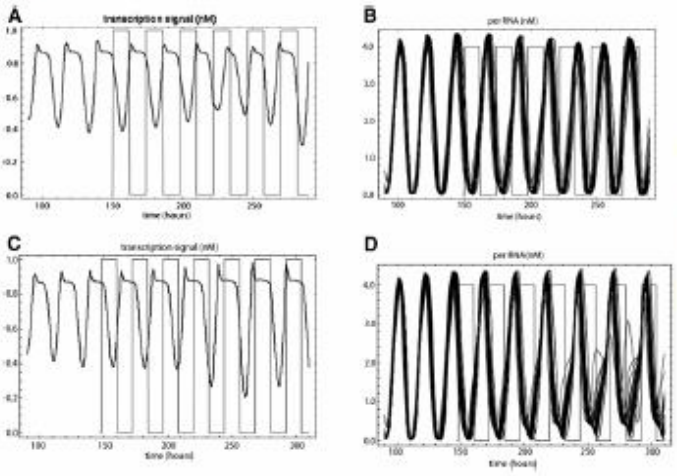

FIGURE 3 Entrainment of the model network to a sequence of 12-12 light-dark cycles. (*A* and *B*) It takes ~6 days to phase-advance by −12 h to entrain the transcription signal (*SN*) (*A*) and *per* RNA (*MP*) (*B*). (*C* and *D*) It takes ~7 days for a 10-h phase delay to entrain the transcription signal (*C*) and *per* RNA (*D*). Light periods are shown as sequences of black rectangles and represented by $ptrbR = 0.006$ in Eq. A13 and $ptrbS = 0.006$ in Eq. A14.

high latitudes near an equinox (56). Again, similar to our experimental animals, the model was able to anticipate the expected light and dark edges as it proceeded into constant darkness (Fig. 4, *G* and *H*).

We next reduced the rythmicity of the VIP feedback loop, and this resulted in an immediate large phase shift as the model proceeded into constant darkness, which we interpreted as a loss of cycle memory (Fig. 4 *I*). We tested the opposite effect, reducing the effect of light on a strongly rhythmic VIP oscillation, which markedly increased the duration of cycle memory (Fig. 4 *J*). Thus, it appears that light-dark cycle memory and cycle-rate memory can be accounted for by a strongly rhythmic neuropeptide feedback loop upon which light acts as a perturbation. For memory, what is important is that the light-perturbed VIP limit cycle be similar to the unperturbed cycle. Note that the SCN is ~100 times less sensitive to light than are the retina's rod cells (48). Note also that increasing the coupling strength between light and the SCN will increase the range of entrainment and shorten the acquisition time, but that these changes come at the expense of cycle memory.

DISCUSSION

A strongly nonlinear negative feedback appears to be required to maintain the limit-cycle oscillation in the biochemistry inside an individual clock neuron (24). Leloup and Goldbeter noted that the strong rhythmicity within a clock neuron's repressor feedback loop depended upon a strongly nonlinear negative feedback, characterized by a nonlinear feedback equation that used an exponent significantly greater than 1 ($n = 4$ in Eqs. A1 and A2). This choice made for a robust circadian oscillation of the clock proteins PER and CRY within a single uncoupled clock neuron in constant darkness. Apparently, strong nonlinearities are also required in the coupling pathway between clock neurons to compete against and overcome the cell's own natural rhythm, so as to be able to synchronize clock neurons in constant darkness. Strong nonlinearity within the neuropeptide feedback loop in the synchronization pathway between clock neurons allows for a high-contrast synchronizing signal to be exchanged between them, which then leads to a high degree of synchronization (exponents o in Eq. A1 and p in Eq. A11). Also, a strongly rhythmic VIP oscillation on which light acts only weakly leads functionally to light-dark cycle memory. This can be obtained by making the negative feedback within the loop strongly nonlinear (exponent $p = 4$ in Eq. A11) and also by increasing loop gain ($c4$ in Eq. A11, $c9$ in Eq. A13a, and $c11$ in Eq. A14a).

There is some controversy concerning the intrinsic rhythmicity of clock neurons, whether many remain rhythmic when uncoupled, and whether coupling should convey both synchronicity and rhythmicity upon them (3,23). Indeed, if a particular clock neuron has strong intrinsic rhythmicity with a period length that is several hours distinct from the circadian day then it would seem that a very strong coupling would be required to synchronize it to the day. It is evident that a natural competition should arise between the intrinsic rhythmicity of an individual clock neuron and the rhythmicity of the loop that synchronizes them together. It is possible that many repressor and promoter feedback loops are intentionally made only weakly rhythmic to permit easier synchronization between them.

There is a natural question concerning the multiple actions of the VIP: why should VIPs act quickly to increase firing rate while at the same time inducing clock gene transcription and then later inhibit a clock neuron's own VIP production? Compare the VIP oscillation in the SCN in complete darkness with the voltage oscillation in a hair cell in the frog's hearing organ in complete quiet (57). In the quiet, a current of potassium ions leaks into the hair cell, which depolarizes it and turns on a fast, voltage-gated calcium current that further depolarizes

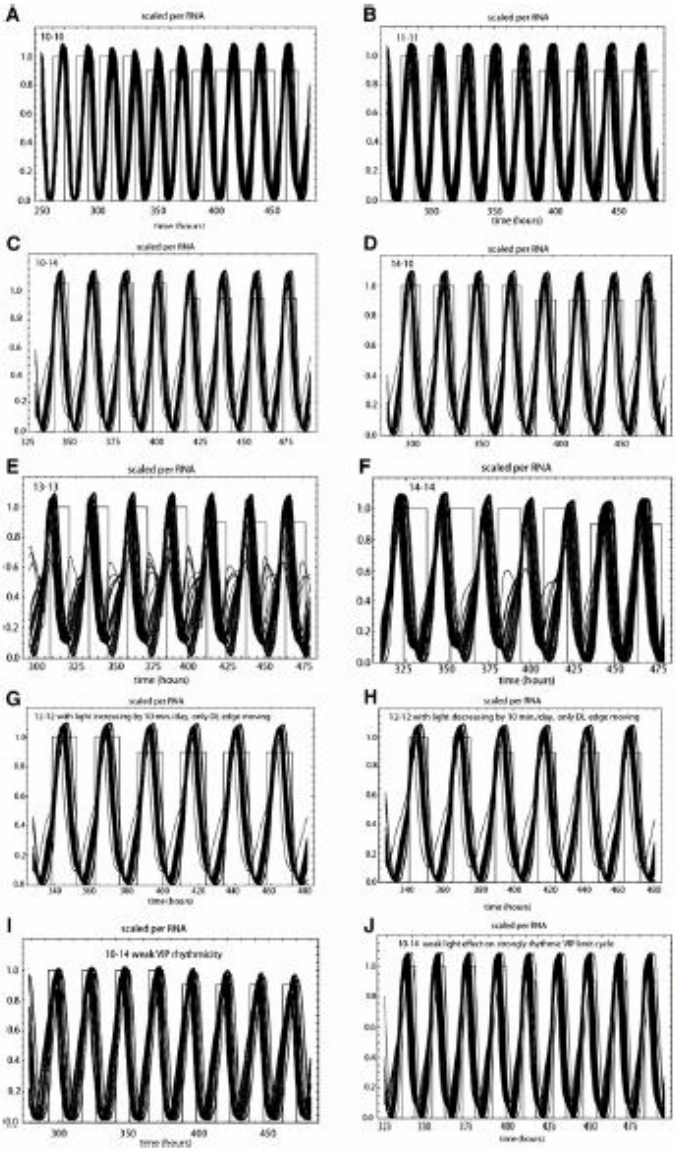

FIGURE 4 Light-dark cycle memory and range of entrainment. *per* RNA (*MP*) is shown for the last several of 12 days of light-dark cycles. Periods of light are indicated by the tall rectangles, whereas the shorter rectangles are in constant darkness and show where the light would be if the cycle were continued. Network phase shifts (PS) for the first several days in constant darkness can be seen by eye, but in the caption we give PS1, 2 and 3 for the first, second and third days in constant darkness with respect to the last day on the light-dark cycle. (*A*) Model with an FRP of 24.0 h was unable to lock a 10-10 cycle. (*B*) The same model as in *A* was able to lock an 11-11 cycle (PS1 = 0, PS2 = −119 min., and PS3 = −200 min). (*C*) Model with a 10-14 cycle had 1 day of memory before the phase advance (PS1 = 0, PS2 = +13 min., and PS3 = +13 min). (*D*) Model with a 14-10 cycle had 1 day of memory before phase delay (PS1 = 0, PS2 = −47 min., and PS3 = −47 min). (*E*) Model with a 13-13 cycle had 1 day of memory before phase advance (PS1 = 0, PS2 = +30 min, and PS3 = +54 min). (*F*) Model was unable to lock a 14-14 cycle. (*G*) Model with a 12-12 cycle whose light was advanced/increased by 10 min/day shows −1 day of cycle-rate memory before phase delay (PS1 = 0, PS2 = −32 min, and PS3 = −47 min). (*H*) Model with a 12-12 cycle whose light period was delayed/decreased by 10 min/day also had 1 day of cycle-rate memory before phase advance (PS1 = 0, PS2 = +32 min, and PS3 = +32 min). (*I*) Memory lost for a 10-14 cycle when rhythmicity of the VIP oscillation was reduced (*c4* 0.37 → 0.36 in Eq. A11; *c9* 1.5 → 1.45 in Eq. A13a; *c11* 2.0 → 1.5 in Eq. A14a; *s* 0.96 → 0.88 to maintain 24.0-h period; PS1 = −15 min., PS2 = −146 min., PS3 = −176 min). (*J*) Duration of cycle memory markedly increased when the effect of light perturbation was decreased (*ptrbR* 0.006 → 0.002 in Eq. A13 and *ptrbS* 0.006 → 0.002 in Eq. A14; PS1 = PS2 = PS3 = 0). It is evident that cycle memory depends on light acting as a small perturbation on a strongly rhythmic underlying limit cycle.

it (fast positive feedback). Calcium then binds with a time delay to a calcium-gated potassium channel, which hyperpolarizes the cell (time-delayed negative feedback). When hyperpolarized, all channels turn off and the leak current then restarts the cycle so that hair cell voltage sinusoidally oscillates by several millivolts in the quiet. Note that if the calcium current were not providing fast positive feedback, the hair cell would not oscillate. Compare this to the neuropeptide oscillation in the SCN in constant darkness: as transmitted VIP increases, the firing rate increases, which then further increases transmitted VIP (fast positive feedback). The received VIP then inhibits VIP production with a time delay (time-delayed negative feedback). Similar to turning off the calcium current in the hair cell, if one reduces the VIP to firing-rate gain then the VIP oscillation can be turned off. In both cases, a fast positive feedback followed by a slow negative one makes for spontaneous oscillation in the quiet or in the dark.

Day length on earth is almost exactly 24 h, with the only change being that hours of light are continually being traded for hours of darkness as we go from summer to winter, and vice versa. At 45° north latitude, our light-dark period changes from 16-8 in the summer to 9-15 in the winter, with

the fastest rate of decrease in light occurring near the fall equinox, where the light period is shortening by ~4 min/day (56). What is the advantage to mammalian life on a rotating world that it be able to remember the light-dark cycle and the rate of change of this light-dark cycle? The SCN is in effect remembering the entraining signal by persisting with a long-lived transient limit cycle in its synchronized repressor feedback loops inside its coupled clock neurons. Here, a comparison to electronics is useful: a second-order lock-in amplifier creates a replica signal at a slowly moving entraining frequency and thereby forms a memory for that entraining signal (58). Then, its replica remains close to its locked frequency in the event of a signal dropout, so that when the signal returns, reacquisition by lock-in or pull-in is very rapid. In a lock-in amplifier, an active high-gain feedback loop is responsible for the long holding times. Also note that a third-order lock-in has frequency-rate memory together with frequency and phase memories. Thus, it appears that it is possible to make a reasonable comparison between the mammalian SCN, with its high-gain VIP feedback loop, and a high loop-gain lock-in amplifier. Here, rapid signal reacquisition in case of a light-dark cycle dropout would seem to be one clear advantage. A second advantage for precisely remembering the location of the light and dark edges would likely be light-noise rejection, so that spurious or unexpected light or dark edges would result in minimal phase shifts. Here, we note that the mammalian SCN has a type 1 PRC with a dead zone that rejects light-noise during the day, unlike simpler life forms with type 0 PRCs that lack a dead zone and thus permit light to phase-shift the organism throughout the day (1). Investigations need to be made into the noise-rejection properties of a type 1 PRC with a dynamic dead zone.

We have shown that Siberian hamsters have several days of memory for a light-dark cycle. Cycle memory appears to be due to a strongly rhythmic VIP oscillation and the dead zone in mammals can result from a strongly nonlinear kinase-phosphatase interaction. A good SCN is an extremely accurate timepiece that is correct to within several minutes out of the 1440 in a day (3). In the way that its clock neurons are intentionally kept in the dark and isolated from spurious light, as well as the way that the biochemical limit cycles of its clock neurons form a replica of a light-dark cycle, and thus retain a memory of the entraining light-dark signal, the mammalian SCN resembles a lock-in amplifier (58).

APPENDIX

A clock neuron is represented by 16 dynamical variables: MP, MC, PC, CC, PCC, PCN, MB, BC, BN, IN, VP, V, R, S, SN, and PH. The first 10 are taken directly from the LG mammalian clock neuron model (24). Below is a list of the 16 differential equations together with three auxiliary equations that represent one clock neuron. The parameters and Mathematica model can be found in the Supporting Material. s is a scale factor that sets the average natural period of the clock neurons, and the random variable s_i scales a particular neuron's repressor and promoter feedback loops to vary this period.

Repressor feedback loop

$$\frac{dMP[t]}{dt} = s\ s_i\left(vsP\ \frac{BN[t]^n}{KAP^n + BN[t]^n} + c1\frac{SN[t]^o}{c2^o + SN[t]^o} - vmP\frac{MP[t]}{KmP + MP[t]} - kdmp\ MP[t]\right) \tag{A1}$$

$$\frac{dMC[t]}{dt} = s\ s_i\left(vsC\frac{BN[t]^n}{KAC^n + BN[t]^n} - vmC\frac{MC[t]}{KmC + MC[t]} - kdmc\ MC[t]\right) \tag{A2}$$

$$\frac{dPC[t]}{dt} = s\ s_i\left(ksP\ MP[t] + k4\ PCC[t] - v1P \times\frac{PC[t]}{Kp + PC[t]} - k3\ PC[t]\ CC[t] - kdpc\ PC[t]\right) \tag{A3}$$

$$\frac{dCC[t]}{dt} = s\ s_i\left(ksC\ MC[t] + k4\ PCC[t] - v1C \times\frac{CC[t]}{Kp + CC[t]} - k3\ PC[t]\ CC[t] - kdcc\ CC[t]\right) \tag{A4}$$

$$\frac{dPCC[t]}{dt} = s\ s_i\left(k3\ PC[t]\ CC[t] + k2\ PCN[t] - V1PC\ \frac{PCC[t]}{Kp + PCC[t]} - k4\ PCC[t] - k1\ PCC[t] - kdpcc\ PCC[t]\right) \tag{A5}$$

$$\frac{dPCN[t]}{dt} = s\ s_i\left(k1\ PCC[t] + k8\ IN[t] - V3PC\ \frac{PCN[t]}{Kp + PCN[t]} - k2\ PCN[t] - k7\ BN[t]\ PCN[t] - kdpcn\ PCN[t]\right) \tag{A6}$$

Promoter feedback loop

$$\frac{dMB[t]}{dt} = s\ s_i\left(vsB\ \frac{KIB^m}{KIB^m + BN[t]^m} - vmB \times\frac{MB[t]}{KmB + MB[t]} - kdmb\ MB[t]\right) \tag{A7}$$

$$\frac{dBC[t]}{dt} = s\ s_i\left(ksB\ MB[t] + k6\ BN[t] - V1B\frac{BC[t]}{Kp\ + BC[t]} - k5\ BC[t]\ - kdbc\ BC[t]\right) \quad \text{(A8)}$$

$$\frac{dBN[t]}{dt} = s\ s_i\left(k5\ BC[t]\ + k8\ IN[t] - V3B\frac{BN[t]}{Kp\ + BN[t]} - k6\ BN[t]\ - k7\ BN[t]\ PCN[t] - kdbn\ BN[t]\right) \quad \text{(A9)}$$

Coupling between repressor and promoter feedback loops

$$\frac{dIN[t]}{dt} = s\ s_i\left(k7\ BN[t]\ PCN[t] - k8\ IN[t] - vdIN\frac{IN[t]}{Kd\ + IN[t]} - kdi\ IN[t]\right) \quad \text{(A10)}$$

VIP feedback loop

$$\frac{dVP[t]}{dt} = s\ \left(c3 - c4\ \frac{SN[t]^p}{c5^p\ + SN[t]^p} - c6\ VP[t]\right) \quad \text{(A11)}$$

$$\frac{dV[t]}{dt} = s\ \left(\frac{VP[t] - V[t]}{tv}\right) \quad \text{(A12)}$$

$$\frac{dR[t]}{dt} = s\ \left(\frac{Rinf[t]\ + ptrbR\quad UnitStep[t - ptrbt]\quad UnitStep[ptrbt\ + step - t] - R[t]}{tR}\right) \quad \text{(A13)}$$

$$Rinf[t] = c8 + c9\ \frac{\sum_{j=1}^{NN}\left(R_j[t]\ V_j[t]\right)}{NN} - c10\ \frac{\sum_{j=1}^{NN}\left(R_j[t]\ V_j[t]\right)^2}{NN} \quad \text{(A13a)}$$

$$\frac{dS[t]}{dt} = s\ \left(\frac{Sinf[t]\ + ptrbS\quad UnitStep[t - ptrbt]\quad UnitStep[ptrbt\ + step - t] - DZ[t] - S[t]}{tS}\right) \quad \text{(A14)}$$

$$Sinf[t] = c11\ \frac{\sum_{j=1}^{NN}\left(R_j[t]\ V_j[t]\right)}{NN} \quad \text{(A14a)}$$

$$DZ[t] = \frac{(S[t]\ PH[t])^q}{c7^q + (S[t]\ PH[t])^q} \quad \text{(A14b)}$$

$$\frac{dSN[t]}{dt} = s\ \left(\frac{S[t] - SN[t]}{tSN}\right) \quad \text{(A15)}$$

Phosphatase

$$\frac{dPH[t]}{dt} = s\left(\frac{SN[t] - PH[t]}{tPH}\right) \quad \text{(A16)}$$

SUPPORTING MATERIAL

The Mathematica model of the ventrolateral SCN is available at http://www.biophysj.org/biophysj/supplemental/S0006-3495(09)01114-X.

We thank the animal care staff at the University of Memphis, and Shing Lam for compiling the C code based on a formula first published by Meeus (56).

Funds were provided by the University of Memphis.

REFERENCES

1. Dunlap, J. C., J. J. Loros, and P. J. Decoursey. 2004. Chronobiology: Biological Timekeeping. Sinauer, Sunderland, MA.
2. Moore, R. Y. 1999. Circadian timing. *In* Fundamental Neuroscience. Michael J. Zigmond, Floyd E. Bloom, Story C. Landis, James L. Roberts, and Larry R. Squire, editors. Academic Press, San Diego, CA. 1198–1206.
3. Aton, S.J., and E. D. Herzog. 2005. Come together, right…now: synchronization of rythms in a mammalian circadian clock. *Neuron.* 48:531–534.
4. Reppert, S. M., and D. R. Weaver. 2002. Coordination of circadian timing in mammals. *Nature.* 418:935–941.
5. Stephan, F. K., and I. Zucker. 1972. Circadian rhythms in drinking behavior and locomotor activity of rats are eliminated by hypothalamic lesions. *Proc. Natl. Acad. Sci. USA.* 69:1583–1586.
6. Welsh, D. K., D. E. Logothetis, M. Meister, and S. M. Reppert. 1995. Individual neurons dissociated from rat superchiasmatic nucleus express independently phased circadian firing rhythms. *Neuron.* 14:697–706.
7. Abrahamson, E. E., and R. Y. Moore. 2001. Suprachiasmatic nucleus in the mouse: retinal innervation, intrinsic organization and efferent projections. *Brain Res.* 916:172–191.
8. Aton, S. J., C. S. Colwell, A. J. Harmar, J. Waschek, and E. D. Herzog. 2005. Vasoactive intestinal polypeptide mediates circadian rhythmicity and synchrony in mammalian clock neurons. *Nat. Neurosci.* 8:476–483.
9. Brown, T. M., A. T. Hughes, and H. D. Piggins. 2005. Gastrin-releasing peptide promotes suprachiasmatic nuclei cellular rhythmicity in the absence of vasoactive intestinal polypeptide-VPAC2 receptor signaling. *J. Neurosci.* 25:11155–11164.
10. Liu, C., and S. M. Reppert. 2000. GABA synchronizes clock cells within the suprachiasmatic circadian clock. *Neuron.* 25:123–128.

11. Maywood, E. S., A. B. Reddy, G. K. Wong, J. S. O'Neill, J. A. O'Brien, et al. 2006. Synchronization and maintenance of timekeeping in suprachiasmatic circadian clock cells by neuropeptidergic signaling. *Curr. Biol.* 16:599–605.
12. Piggins, H. D., M. C. Antle, and B. Rusak. 1995. Neuropeptides phase shift the mammalian circadian pacemaker. *J. Neurosci.* 15:5612–5622.
13. Reed, H. E., A. Meyer-Spasche, D. J. Cutler, C. W. Coen, and H. D. Piggins. 2001. Vasoactive intestinal polypeptide (VIP) phase-shifts the rat suprachiasmatic nucleus clock in vitro. *Eur. J. Neurosci.* 13:839–843.
14. Shen, S., C. Spratt, W. J. Sheward, I. Kallo, K. West, et al. 2000. Overexpression of the human VPAC2 receptor in the suprachiasmatic nucleus alters the circadian phenotype of mice. *Proc. Natl. Acad. Sci. USA.* 97:11575–11580.
15. Harmar, A. J., H. M. Marston, S. Shen, C. Spratt, K. M. West, et al. 2002. The VPAC(2) receptor is essential for circadian function in the mouse suprachiasmatic nuclei. *Cell.* 109:497–508.
16. Itri, J., and C. S. Colwell. 2003. Regulation of inhibitory synaptic transmission by vasoactive intestinal peptide (VIP) in the mouse suprachiasmatic nucleus. *J. Neurophysiol.* 90:1589–1597.
17. Aton, S. J., J. E. Huettner, M. Straume, and E. D. Herzog. 2006. GABA and $G_{i/o}$ differentially control circadian rhythms and synchrony in clock neurons. *Proc. Natl. Acad. Sci. USA.* 103:19188–19193.
18. Strogatz, S. 1987. Human sleep and circadian rythms: a simple model based on two coupled oscillators. *J. Math. Biol.* 25:327–347.
19. Garcia-Ojalvo, J., M. B. Elowitz, and S. H. Strogatz. 2004. Modeling a synthetic multicellular clock: repressilators coupled by quorum sensing. *Proc. Natl. Acad. Sci. USA.* 101:10955–10960.
20. Antle, M. C., D. K. Foley, N. C. Foley, and R. Silver. 2003. Gates and oscillators: a network model of the brain clock. *J. Biol. Rhythms.* 18:339–350.
21. Gonze, D., S. Bernard, C. Waltermann, A. Kramer, and H. Herzel. 2005. Spontaneous synchronization of coupled circadian oscillators. *Biophys. J.* 89:120–129.
22. Bernard, S., D. Gonze, B. Cajavec, H. Herzel, and A. Kramer. 2007. Synchronization-induced rythmicity of circadian oscillators in the suprachiasmatic nucleus. *PLOS Comput. Biol.* 3:667–679.
23. To, T.-L., M. A. Hensen, E. D. Herzog, and F. J. Doyle, III. 2007. A molecular model for intercellular synchronization in the mammalian circadian clock. *Biophys. J.* 92:3792–3803.
24. Leloup, J.-C., and A. Goldbeter. 2003. Toward a detailed computational model for the mammalian circadian clock. *Proc. Natl. Acad. Sci. USA.* 100:7051–7056.
25. Forger, D. B., and C. S. Peskin. 2003. A detailed predictive model of the mammalian circadian clock. *Proc. Natl. Acad. Sci. USA.* 100:14806–14811.
26. Forger, D. B., and C. S. Peskin. 2005. Stochastic simulation of the mammalian circadian clock. *Proc. Natl. Acad. Sci. USA.* 102:321–324.
27. Leloup, J.-C., and A. Goldbeter. 2004. Modeling the mammalian circadian clock: sensitivity analysis and multiplicity of oscillatory mechanisms. *J. Theor. Biol.* 230:541–562.
28. Hao, H., D. E. Zak, T. Sauter, J. Schwaber, and B. A. Ogunnaike. 2006. Modeling the $VPAC_2$-activated cAMP/PKA signaling pathway: from receptor to circadian clock gene induction. *Biophys. J.* 90:1560–1571.
29. Forger, D. B., D. Gonze, D. Virshup, and D. K. Welsh. 2007. Beyond intuitive modeling: combining biophysical models with innovative experiments to move the circadian clock field forward. *J. Biol. Rhythms.* 22:200–210.
30. Indic, P., W. J. Schwartz, E. D. Herzog, N. C. Foley, and M. C. Antle. 2007. Modeling the behavior of coupled cellular circadian oscillators in the superchiasmatic nucleus. *J. Biol. Rhythms.* 22:211–219.
31. Yamaguchi, S., H. Isejima, T. Matsuo, R. Okura, K. Yagita, et al. 2003. Synchronization of cellular clocks in the suprachiasmatic nucleus. *Science.* 302:1408–1412.
32. Shinohara, K., S. Honma, Y. Katsuno, H. Abe, and K. Honma. 1995. Two distinct oscillators in the rat suprachiasmatic nucleus. *Proc. Natl. Acad. Sci. USA.* 92:7396–7400.
33. Yin, L., J. Wang, P. S. Klein, and M. A. Lazar. 2006. Nuclear receptor Reverbα is a critical lithium-sensitive component of the circadian clock. *Science.* 311:1002–1005.
34. Harada, Y., M. Sakai, N. Kurabayashi, T. Hirota, and Y. Fukada. 2005. Ser-557-phosphorylated mCRY2 is degraded upon synergystic phosphorylation by glycogen synthase kinase-3β. *J. Biol. Chem.* 280:31714–31721.
35. Iitaka, C., K. Miyazaki, T. Akaike, and N. Ishida. 2005. A role for glycogen synthase kinase-3β in the mammalian circadian clock. *J. Biol. Chem.* 280:29397–29402.
36. Shinohara, K., K. Tominaga, Y. Isobe, and S.-I. T. Inouye. 1993. Photic regulation of peptides located in the ventrolateral subdivision of the suprachiasmatic nucleus of the rat: daily variations of vasoactive intestinal polypeptide, gastrin-releasing peptide, and neuropeptide Y. *J. Neurosci.* 13:793–800.
37. Zylka, M. J., L. P. Shearman, D. R. Weaver, and S. M. Reppert. 1998. Three period homologs in mammals: differential light responses in the suprachiasmatic circadian clock and oscillating transcripts outside of the brain. *Neuron.* 20:1103–1110.
38. Doi, M., S. Cho, I. Yujnovsky, J. Hirayama, N. Cermakian, et al. 2007. Light-inducible and clock-controlled expression of MAP kinase phosphatase 1 in mouse central pacemaker neurons. *J. Biol. Rhythms.* 22:127–139.
39. Reference deleted in proof.
40. Pakhotin, P., A. J. Harmar, A. Verkhratsky, and H. Piggins. 2006. VIP receptors control excitability of suprachiasmatic nuclei neurons. *Eur. J. Phys.* 452:7–15.
41. Pennartz, C. M. A., M. T. G. De Jeu, N. P. A. Bos, J. Schaap, and A. M. S. Geurtsen. 2002. Diurnal modulation of pacemaker potentials and calcium current in the mammalian circadian clock. *Nature.* 416:286–290.
42. Ikeda, M., T. Sugiyama, C. S. Wallace, H. S. Gompf, T. Yoshioka, et al. 2003. Circadian dynamics of cytosolic and nuclear Ca^{++} in single suprachiasmatic nucleus neurons. *Neuron.* 38:253–263.
43. Pizzio, G. A., E. C. Hainich, G. A. Ferreyra, O. A. Coso, and D. A. Golombek. 2003. Circadian and photic regulation of ERK, JNK and p38 in the hamster SCN. *Neuroreport.* 14:1417–1419.
44. Vosko, A. M., A. Schroeder, D. H. Loh, and C. S. Colwell. 2007. Vasoactive intestinal peptide and the mammalian circadian system. *Gen. Comp. Endocrinol.* 152:165–175.
45. Maywood, E., J. O'Neill, J. E. Chesham, and M. H. Hastings. 2007. Minireview: the circadian clockwork of the suprachiasmatic nuclei: analysis of a cellular oscillator that drives endocrine rhythms. *Endocrinology.* 148:5624–5634.
46. Travnickova-Bendova, Z., N. Cermakian, S. M. Reppert, and P. Sassone-Corsi. 2002. Bimodal regulation of mPeriod promoters by CREB-dependent signaling and CLOCK/BMAL1 activity. *Proc. Natl. Acad. Sci. USA.* 99:7728–7733.
47. Meijer, J. H., K. Watanabe, J. Schaap, H. Albus, and L. Detari. 1998. Light responsiveness of the suprachiasmatic nucleus: long-term multiunit and single-unit recordings in freely moving rats. *J. Neurosci.* 18:9078–9087.
48. Nakamura, T. J., K. Fujimura, S. Ebihara, and K. Shinohara. 2004. Light response of the neuronal firing activity in the suprachiasmatic nucleus of mice. *Neurosci. Lett.* 371:244–248.
49. Strogatz, S. 1994. Nonlinear Dynamics and Chaos. Perseus Books, Reading, MA.
50. Buck, J. 1988. Synchronous rhythmic flashing of fire flies, part II. *Q. Rev. Biol.* 63:265–289.
51. Strogatz, S. 2003. Sync: How Order Emerges from Chaos in the Universe, Nature, and Daily Life. Hyperion Press, New York.

52. Puchalski, W., and G. R. Lynch. 1992. Relationship between phase resetting and the free-running period in Djungarian hamsters. *J. Biol. Rhythms*. 7:75–83.

53. Colwell, C. S., S. Michel, J. Itri, W. Rodriguez, J. Tam, et al. 2004. Selective deficits in the circadian light response in mice lacking PACAP. *Am. J. Physiol.* 287:R1194–R1201.

54. Leloup, J.-C., and A. Goldbeter. 1998. A model for circadian rhythms in *Drosophila* incorporating the formation of a complex between the PER and TIM proteins. *J. Biol. Rhythms*. 13:70–87.

55. Theodosiou, A., and A. Ashworth. 2002. MAP kinase phosphatases. *Genome Biol*. 3 Reviews3009:1–10.

56. Meeus, Jean. 1991. Astronomical Algorithms. Willmann-Bell, Richmond, VA.

57. Ospeck, M., V. M. Eguiluz, and M. O. Magnasco. 2001. Evidence of a Hopf bifurcation in frog hair cells. *Biophys. J.* 80:2597–2607.

58. Gardner, F. M. 1979. Phaselock Techniques, 2nd ed. John Wiley and Sons, New York.